The MIDAS Touch: Accurate and Scalable Missing-Data Imputation with Deep Learning

Ranjit Lall* Thomas Robinson†

January 14, 2021

Forthcoming, *Political Analysis*

Abstract

Principled methods for analyzing missing values, based chiefly on multiple imputation, have become increasingly popular yet can struggle to handle the kinds of large and complex data that are also becoming common. We propose an accurate, fast, and scalable approach to multiple imputation, which we call MIDAS (Multiple Imputation with Denoising Autoencoders). MIDAS employs a class of unsupervised neural networks known as denoising autoencoders, which are designed to reduce dimensionality by corrupting and attempting to reconstruct a subset of data. We repurpose denoising autoencoders for multiple imputation by treating missing values as an additional portion of corrupted data and drawing imputations from a model trained to minimize the reconstruction error on the originally observed portion. Systematic tests on simulated as well as real social science data, together with an applied example involving a large-scale electoral survey, illustrate MIDAS's accuracy and efficiency across a range of settings. We provide open-source software for implementing MIDAS.

*London School of Economics and Political Science. Email: r.lall@lse.ac.uk.
†Durham University. Email: thomas.robinson@durham.ac.uk.

1 Introduction

Across a variety of disciplines, the analysis of data with missing values has recently been characterized by two trends that have yet to be reconciled. First, to avoid the problems caused by popular ad-hoc methods such as listwise deletion (discarding rows of the dataset that contain any missing values), analysts are increasingly turning to principled techniques for imputing, or filling in, missing values recommended by the statistics community. The most widely used of these techniques, multiple imputation (MI), involves replacing each missing element with several values that preserve relationships within the observed data while representing uncertainty about the correct value. In the words of a prominent scholar of missing-data analysis, "[MI] is now accepted as the best general method to deal with incomplete data in many fields" (van Buuren 2012, 25).

Second, advances in computational power, efficiency, and storage capacity have enabled the compilation and analysis of unprecedentedly large and complex datasets, ushering in an era of so-called "Big Data." While massively increasing the amount of information available for analysis, however, this development has not eliminated the problem of missing data. That is, bigger data has not necessarily translated into more *complete* data.

The growing scale and complexity of data present a computational challenge for existing MI algorithms, which were generally designed for small or medium-sized applications with relatively simple (mostly linear) structures. While working well in many settings, these algorithms can suffer from performance problems when applied to larger datasets with features such as high dimensionality, severe nonlinearities, and unconventional func-

tional forms. Convergence failures and slow — sometimes prohibitive — runtimes become increasingly common, with imputations more likely to take on extreme and unusual values. Analysts can thus face an unappealing choice: limit the size or complexity of the data passed into the MI algorithm, risking bias and reducing statistical efficiency; or employ an ad-hoc method that *can* be applied to the original data, such as listwise deletion or mean imputation (replacing missing data with observed column averages), creating an even greater risk of bias and guaranteeing inefficiency (Little and Rubin 1987, Ch. 3-4).[1]

This article proposes an accurate, fast, and scalable approach to MI, which we call MIDAS (Multiple Imputation with Denoising Autoencoders). MIDAS employs a class of unsupervised neural networks known as denoising autoencoders (DAs), which were recently developed to optimize the task of dimensionality reduction. DAs corrupt a subset of input data via the injection of stochastic noise and attempt to reconstruct it through a series of nested nonlinear transformations. The key innovation in MIDAS is to treat missing values as an additional portion of corrupted data and thus draw imputations from a model trained to minimize the reconstruction error on the originally observed portion. To reduce the risk of overfitting, we train this imputation-repurposed DA with the technique of dropout, which extends the corruption process deeper into the neural network architecture. With the combination of denoising and dropout, MIDAS employs an effectively

[1]For instance, using the popular **Amelia** package in `R` (Honaker et al. 2011) to reanalyze the results of a large number of political science articles, Lall (2016) has to restrict the size of imputation model and reduce variance in the data to consistently avoid convergence problems. We provide further illustrations of this dilemma below.

nonparametric imputation model that places constraints not on the joint distribution of the data — the standard approach to MI — but only on the distribution of possible *functions* that characterize the data. Functional flexibility enables the model to capture simple as well as highly complex relationships between variables, providing the basis for performance gains across diverse data types and structures. This flexibility, we believe, makes MIDAS a useful complement to existing MI strategies in a wide range of fields where large and complex data are becoming common, including political science, economics, public health, computer science, and other parts of the social and natural sciences.

To implement MIDAS, we develop an efficient algorithm that expands the range and quantity of data that can be analyzed with MI. This procedure leverages the powerful and flexible computational architecture of the **TensorFlow** programming platform, allowing a wide variety of data types and supporting high degrees of parallelization on supported systems. As a companion to this article, we make the algorithm available in an easy-to-use `Python` class (**MIDASpy**) and `R` package (**rMIDAS**) — the first full-featured, open-source software for performing MI with neural network technology.[2]

We illustrate MIDAS's accuracy and scalability through a series of systematic tests involving real as well as simulated data.[3] We first conduct two Monte Carlo simulation experiments that assess MIDAS's accuracy under the statistical conditions assumed by the

[2]**MIDASpy** can be installed from PyPI, **rMIDAS** from CRAN. For further information, see `https://github.com/MIDASverse`.

[3]Data and code for replicating the results of these tests are provided in Lall and Robinson (2020).

dominant approach to MI, namely, joint multivariate normality. The first experiment establishes that MIDAS yields accurate estimated posterior densities and confidence intervals for linear regression coefficients, while the second shows that the accuracy of MIDAS's imputed values and parameter estimates compares favorably with that of leading existing MI algorithms. We then move to a more realistic setting, introducing varying levels and patterns of missingness into a widely used census dataset. We find that MIDAS yields more accurate imputed values than other MI algorithms across most missingness conditions, even performing well under patterns where MI cannot avoid some degree of bias.

We test MIDAS's scalability by sampling increasing numbers of rows and columns from a popular electoral survey that typifies the kind of large and complex data analyzed by political scientists. MIDAS produces completed datasets in consistently less time than existing MI algorithms, with the gap increasing linearly with the number of rows and exponentially with the number of columns. Even with modestly-sized datasets, MIDAS's efficiency translates into substantial time savings for analysts. For datasets approaching the dimensions of modern Big Data, where existing MI algorithms can be impractically slow, it may make the difference between employing a principled and valid approach to analyzing missing data and resorting to an ad-hoc method that results in biased and inefficient inferences.

Finally, we provide an applied illustration of MIDAS's capacity to handle datasets that pose computational problems for existing MI algorithms — that is, to give us access to new substantive knowledge — that involves estimating the latent ideology of participants in the electoral survey used in the scalability test. We show that substituting MIDAS for

listwise deletion, which enables us to recover estimates for more than 10,000 additional respondents, materially alters our understanding of the distribution of latent ideology in the sample and of the relationship between this variable and presidential job approval.

2 MIDAS: Theory and Implementation

2.1 Multiple Imputation

The first building block of MIDAS, MI, consists of three steps: (1) replacing each missing element in the dataset with M independently drawn imputed values that preserve relationships expressed by observed elements; (2) analyzing the M completed datasets separately and estimating parameters of interest; and (3) combining the M separate parameter estimates using a simple set of rules that leverages variation across these datasets to reflect our uncertainty about the correct imputation model.[4]

The dominant approach to MI assumes that the complete data follow a multivariate normal distribution, which implies that each variable is continuous and a linear function of all others (e.g., King et al. 2001; Honaker and King 2010). An alternative approach models each variable's distribution conditionally on all others in an iterative fashion, typically using a generalized linear estimator, which allows for a wider class of variable types and distributions (e.g., Kropko et al. 2014). Imputed values, however, need not be drawn

[4]These rules, which are described in Rubin (1987), involve averaging the M parameter estimates and computing variance as a weighted sum of the estimated variance within and between the M datasets.

from a posterior density. A notable nonparametric approach is predictive mean matching, which involves replacing missing values with observed ones from similar rows (according to a chosen metric) (e.g., Cranmer and Gill 2013).

All approaches to MI share three attractive features. First, they yield unbiased estimates of parameters in the subsequent analytical model (e.g., regression coefficients) under a fairly wide range of statistical conditions: data are either *missing completely at random* (MCAR), i.e., the pattern of missingness is independent of observed and missing data, or *missing at random* (MAR), i.e., this pattern depends on observed data. They cannot avoid bias when data are *missing not at random* (MNAR), i.e., missingness depends on missing data, though can still perform well if the observed data include strong predictors of missingness (Lall 2016).[5] Second, they tend to result in more efficient estimators than methods that do not utilize all observed values (such as listwise deletion). Third, from a practical perspective, they are simple to implement because they do not require directly modeling the missingness mechanism and, due to the separation between imputation and analysis, can be combined with standard complete-data methods.

Although useful in many settings, existing approaches to MI also have a common limitation: they can perform poorly with the kinds of large and complex data that are becoming common. This is in part because extreme departures from their assumptions occur more frequently in these data and in part due to problems of computational implementation. Most approaches are implemented with a variant of either the imputation-posterior algorithm, which draws missing values from the appropriate posterior distribution using

[5]For formal definitions of these missingness mechanisms, see Little and Rubin (1987).

Markov chain Monte Carlo (MCMC) methods, or the expectation-maximization algorithm, a similar procedure that substitutes maximum likelihood estimates for posterior draws. For a variety of reasons — including their serial nature, sweep of the entire dataset at each iteration, and simultaneous updating of all parameters — both algorithms "have well-known problems with large data sets. . .creating unacceptably long run-times or software crashes" (Honaker and King 2010, 564). Even when they do converge, they can fail to accurately approximate posteriors due to local maxima or major divergence from the assumed joint distribution. Some approaches seek to overcome these problems by combining one of the above algorithms with bootstrapping. As each bootstrapped sample is the same size as the original dataset, however, these routines can also slow down sharply or fail to converge when applied to large datasets. We later provide evidence of these scalability issues.

2.2 Denoising Autoencoder Neural Networks

MIDAS implements MI with the aid of artificial neural networks, a concept inspired by the structure of the human brain that has been used to enhance the accuracy and efficiency of a wide array of computational tasks. A neural network consists of a series of nested nonlinear functions usually depicted as interconnected nodes organized in layers. Input data are fed into the network through an *input layer*, processed by nodes in one or more *hidden layers*, and returned via nodes in an *output layer*. To more precisely describe these models, we adopt the linear algebraic notation typically used in the machine learning literature, which allows for concise expression of deeply nested functions: italicized

upper-case symbols denote random vectors (e.g., X); bold lower-case symbols ($\mathbf{x}$) denote ordinary column vectors, i.e., realizations of random vectors; bold upper-case symbols denote matrices, with $\mathbf{D} = \{\mathbf{D}_{obs}, \mathbf{D}_{mis}\}$ denoting a dataset in which $\mathbf{D}_{obs}$ is observed and $\mathbf{D}_{mis}$ is missing; and superscripts in parentheses index hidden layers of a network.

The model for a "forward pass" — or computation of output values given input data — through layer h of a neural network is:

$$\mathbf{y}^{(h)} = \sigma(\mathbf{W}^{(h)}\mathbf{y}^{(h-1)} + \mathbf{b}^{(h)}) \tag{1}$$

where $\mathbf{y}^{(h)}$ is a vector of outputs from layer h ($\mathbf{y}^{(0)} = \mathbf{x}$ is the input), $\mathbf{W}^{(h)}$ is a matrix of weights connecting the nodes in layer $h-1$ with the nodes in layer h, $\mathbf{b}$ is a vector of biases for layer h, and σ is a nonlinear activation function. The introduction of nonlinearity into the model enables neural networks to efficiently learn complex functional forms with few hidden layers. This model can be generalized to an arbitrary number of hidden layers H:

$$\mathbf{y} = \Phi(\mathbf{W}^{(H)}[...[\sigma(\mathbf{W}^{(2)}[\sigma(\mathbf{W}^{(1)}\mathbf{x} + \mathbf{b}^{(1)})] + \mathbf{b}^{(2)})]...] + \mathbf{b}^{(H)}) \tag{2}$$

where $\mathbf{x}$ is a vector of inputs and Φ is a final-layer activation function that returns outputs with the appropriate distribution.

The parameters of the network (θ) are weights and biases, which are trained to minimize a loss function $L(\mathbf{y}, \hat{\mathbf{y}})$ that measures the distance between actual and predicted outputs. Training involves four steps, collectively known as an *epoch*, which are repeated until some convergence criterion is met: (1) performing a forward pass through the network using current θ; (2) calculating L; (3) using the chain rule to calculate error gradients with

respect to weights in each layer, a technique called backpropagation; and (4) adjusting weights in the direction of the negative gradient for the next forward pass. Characteristics such as the number of training cycles per epoch, which are specified by the analyst rather than learned in training, are referred to as *hyperparameters*.

One class of neural networks that is naturally suited to the task of imputing missing data is the DA, an extension of the classical autoencoder — a well-established tool for dimensionality reduction in machine learning — proposed by Vincent et al. (2008). Classical autoencoders consist of two parts. First, an *encoder* deterministically maps an input vector $\mathbf{x}$ to a lower-dimensional representation $\mathbf{y}$ by compressing it through a series of shrinking hidden layers that culminate in a "bottleneck" layer (indexed by B):

$$\mathbf{y} = f_\theta(\mathbf{x}) = \sigma(\mathbf{W}^{(B)}[...[\sigma(\mathbf{W}^{(2)}[\sigma(\mathbf{W}^{(1)}\mathbf{x} + \mathbf{b}^{(1)})] + \mathbf{b}^{(2)})]...] + \mathbf{b}^{(B)}) \tag{3}$$

Second, a *decoder* maps $\mathbf{y}$ back to a reconstructed vector $\mathbf{z}$ with the same probability distribution and dimensions as $\mathbf{x}$ by passing it through a parallel series of expanding hidden layers culminating in the output layer:

$$\mathbf{z} = g_{\theta'}(\mathbf{y}) = \Phi(\mathbf{W}^{(H)\prime}[...[\sigma(\mathbf{W}^{(B+2)\prime}[\sigma(\mathbf{W}^{(B+1)\prime}\mathbf{y} + \mathbf{b}^{(B+1)\prime})] + \mathbf{b}^{(B+2)\prime})]...] + \mathbf{b}^{(H)\prime}) \tag{4}$$

To map $\mathbf{z}$ as closely as possible to $\mathbf{x}$, weights are adjusted by backpropagation to minimize a loss function $L(\mathbf{x}, \mathbf{z})$. This process yields a latent representation that captures the key axes of variation in $\mathbf{x}$ in a similar manner to principal component analysis.

DAs were developed to prevent autoencoders from learning an identical representation of the input (the identity function) while enabling them to extract more robust features

from the data, that is, features that generalize better to new samples from the same data-generating process. They achieve these benefits by partially corrupting inputs through the injection of stochastic noise: $\mathbf{x} \rightarrow \tilde{\mathbf{x}} \sim q_D(\mathbf{x}|\tilde{\mathbf{x}})$. The corrupted input is then mapped to a hidden representation $\mathbf{y} = f_\theta(\tilde{\mathbf{x}})$, from which a clean or "denoised" version $\mathbf{z} = g_{\theta'}(\mathbf{y})$ is reconstructed. Unlike before, however, $\mathbf{z}$ is now a deterministic function of $\tilde{\mathbf{x}}$ (not $\mathbf{x}$).

The most common corruption process involves setting a random subset of inputs to 0.[6] In attempting to recover these elements, the DA effectively performs a form of imputation: predicting corrupted (missing) elements based on relationships among uncorrupted (observed) elements. That is, missing values can be seen as a special case of corrupted input data. Building on this insight, recent studies have developed application-specific models for imputing missing values with DAs, reporting impressive performance (e.g., Beaulieu-Jones and Greene 2016; Duan et al. 2014). These studies, however, neither offer a general model of DA-based imputation nor combine DAs with MI, forgoing the latter's advantages vis-á-vis single imputation in bias reduction, efficiency, and uncertainty representation.

To our knowledge, the only existing attempt to implement MI using DAs comes from Gondara and Wang (2018), who propose a model in which data are provisionally completed using mean or mode imputation before being corrupted and passed into the DA.[7] While Gondara and Wang offer a relatively brief overview of their approach, it appears

[6]The value assigned to corrupted data points is not substantively important; 0 is a popular choice because it is often close to the "true" value being estimated, minimizing the adjustment to network parameters in training and hence accelerating model convergence.
[7]We developed MIDAS without knowledge of Gondara and Wang's research.

to suffer from three limitations. First, its loss functions fail to distinguish between originally observed and originally missing values, causing reconstruction error to be measured against the mean/mode imputations, which typically lead to biased parameter estimates. Second, it injects stochastic noise into inputs once rather than in each training epoch, increasing the risk of overfitting and reducing model robustness. Third, instead of sampling from a single trained network, it trains a different network for each set of imputations, substantially slowing runtime — storing all trained models and imputations in memory is computationally demanding — without improving performance. In the rest of the section, we present an alternative approach to MI based on DAs that avoids these issues.

2.3 The MIDAS Model

MIDAS modifies the standard DA model in two key ways. First, as part of the initial corruption process, it forces all missing values — in addition to a random subset of inputs — to 0. The task of the DA is thus to predict corrupted values that were both originally missing ($\tilde{\mathbf{x}}_{\text{mis}}$) and originally observed ($\tilde{\mathbf{x}}_{\text{obs}}$) using a loss function that only includes the latter. Second, to further reduce the risk of overfitting, MIDAS regularizes the DA with the complementary technique of dropout. Introduced by Hinton et al. (2012), dropout involves randomly removing (or "dropping") nodes in the hidden layers of a network during training, typically by multiplying outputs from each of these layers by a Bernoulli vector $\mathbf{v}$ that takes a value of 1 with probability p: $\tilde{\mathbf{y}}^{(h)} = \mathbf{v}^{(h)}\mathbf{y}^{(h)}, \mathbf{v}^{(h)} \sim \text{Bernoulli}(p)$. Dropout is thus a generalization of the idea behind DAs, extending stochastic corruption to the hidden

Figure 1. MIDAS Neural Network Architecture

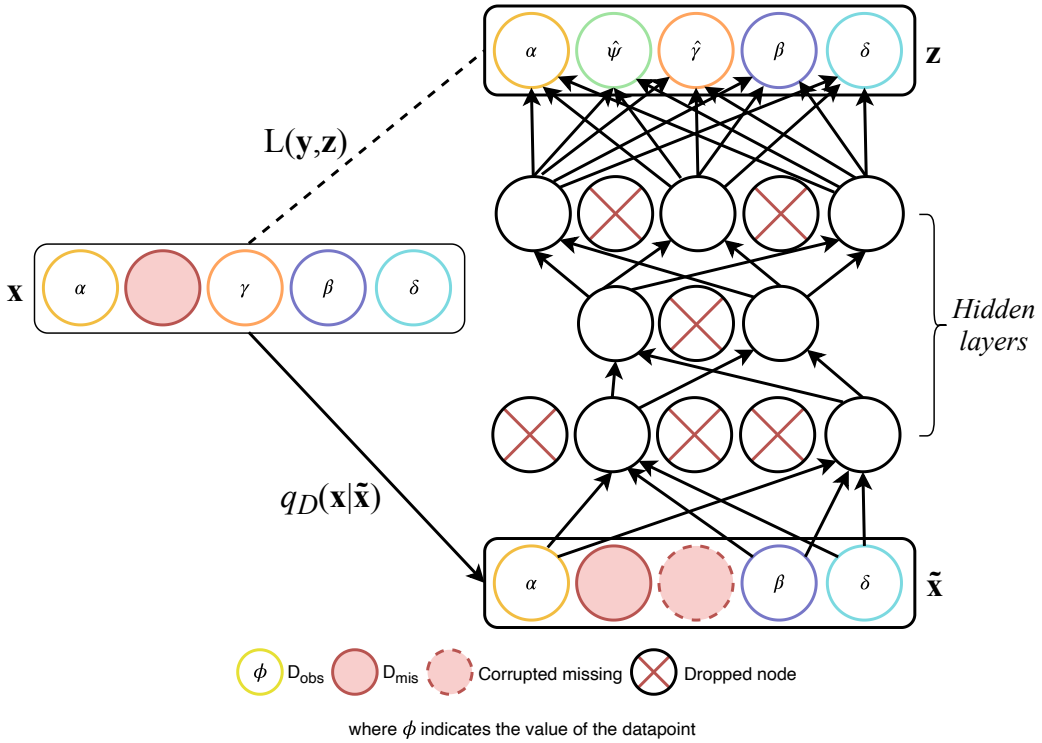

$\mathbf{x}$ is a vector of inputs, $q_D(\mathbf{x}|\tilde{\mathbf{x}})$ is the corruption process, and $\mathbf{z}$ is the "denoised" version of $\tilde{\mathbf{x}}$.

layers and hence enabling the extraction of even more robust features.

Dropout training proceeds by sampling an arbitrary number of "thinned" networks, with a different set of nodes dropped in each iteration. At test time, Hinton et al. propose scaling the weights of a single unthinned network by the probability that their originating nodes were retained during training. To produce *multiple* imputations, MIDAS instead samples M thinned networks. This procedure has recently received a powerful independent justification from Gal and Ghahramani (2016), who show through simulation experiments that it results in more accurate parameter estimation with no additional model complexity or training time. Notably, they also prove that dropout training is math-

ematically equivalent to a Bayesian variational approximation of a Gaussian process (GP), a commonly used probability distribution over functions. The implication is that MIDAS posits not a joint distribution of the data but a distribution over possible functions that describe the data. Since GP models can estimate any continuous function arbitrarily well — they are usually considered nonparametric because they have a potentially infinite number of parameters — MIDAS can thus capture a wider class of joint distributions than existing approaches to MI without making any additional parametric assumptions.

The encoder of an imputation-generating DA trained with dropout — a MIDAS network — can thus be described as:

$$\tilde{\mathbf{y}} = f_\theta(\tilde{\mathbf{x}}) = \sigma(\mathbf{W}^{(B)}\mathbf{v}^{(B)}[...[\sigma(\mathbf{W}^{(2)}\mathbf{v}^{(2)}[\sigma(\mathbf{W}^{(1)}\tilde{\mathbf{x}} + \mathbf{b}^{(1)})] + \mathbf{b}^{(2)})]...] + \mathbf{b}^{(B)}). \quad (5)$$

The decoder, in turn, becomes:

$$\mathbf{z} = g_{\theta'}(\tilde{\mathbf{y}}) = \Phi(\mathbf{W}^{(H)\prime}[...[\sigma(\mathbf{W}^{(B+2)\prime}[\sigma(\mathbf{W}^{(B+1)\prime}\tilde{\mathbf{y}} + \mathbf{b}^{(B+1)\prime})] + \mathbf{b}^{(B+2)\prime})]...] + \mathbf{b}^{(H)\prime}) \quad (6)$$

where $g \dot{\sim}$ GP and $\mathbf{z}$ represents a fully observed vector containing predictions of $\tilde{\mathbf{x}}_{\text{obs}}$ and $\tilde{\mathbf{x}}_{\text{mis}}$. To produce a completed dataset, predictions of $\tilde{\mathbf{x}}_{\text{mis}}$ are substituted for $\mathbf{x}_{\text{mis}}$ in $\mathbf{D}$. The full architecture of a MIDAS network is illustrated in Figure 1.[8]

The default activation function in MIDAS is exponential linear unit (ELU), which is known to facilitate efficient training in deep neural networks. The final-layer activation function is chosen according to the distribution of the input data $\mathbf{x}$, with identity, logistic,

[8]A more detailed description of the MIDAS model's objective function is provided in Online Appendix 2A.

and softmax functions assigned to continuous, binary, and categorical variables, respectively. Loss functions take the same form as in a regular DA, measuring the distance between $\mathbf{x}$ and $\mathbf{z}$: $L(\mathbf{x}, \mathbf{z})$. As we are only interested in the reconstruction error for predictions of originally observed corrupted values ($\tilde{\mathbf{x}}_{\text{obs}}$), however, these functions are multiplied by a missingness indicator vector $\mathbf{r}$. MIDAS employs root mean squared error (RMSE) and cross-entropy loss functions for continuous and categorical variables, respectively:

$$L(\mathbf{x}, \mathbf{z}, \mathbf{r}) = \begin{cases} [\frac{1}{J} \sum_{j=1}^{J} \mathbf{r}_j (\mathbf{x}_j - \mathbf{z}_j)^2]^{\frac{1}{2}} & \text{if } \mathbf{x} \text{ is continuous} \\ -\frac{1}{J} \sum_{j=1}^{J} \mathbf{r}_j [\mathbf{x}_j \log \mathbf{z}_j + (1 - \mathbf{x}_j) \log(1 - \mathbf{z}_j)] & \text{if } \mathbf{x} \text{ is categorical.} \end{cases} \tag{7}$$

In sum, unlike most existing approaches to MI, MIDAS does not assume a joint distribution of the data and use an iterative method to draw imputed values from the posterior of this distribution. Rather, it uses a neural network to "learn" the form of the data by fitting a series of nonlinear functions — in effect, a nonparametric model that only constrains the range of functions that are consistent with the data — which enables it to capture both simple and highly complex patterns. This is implemented by introducing additional missingness into the data during training, minimizing the reconstruction error for predictions of these corrupted values, and drawing imputations from the trained network.

2.4 Algorithm

The algorithm we have developed to implement MIDAS takes an incomplete dataset $\mathbf{D}$ as its input and returns M completed datasets. The algorithm proceeds in three stages, each comprising a number of smaller steps. In the first stage, the input data $\mathbf{D}$ are prepared for

Figure 2. Schematic of MIDAS Training Steps

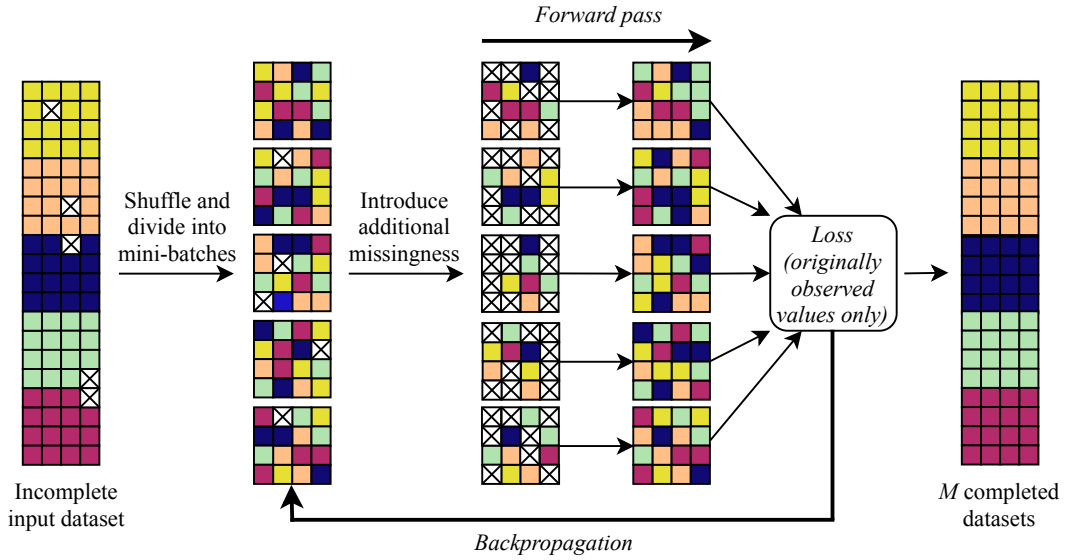

Shaded blocks represent data points (shades denote different variables); crosses indicate missing values.

training. Categorical variables are "one-hot" encoded (i.e., converted into separate dummy variables for each unique class) and continuous variables are rescaled between 0 and 1 to improve convergence. In addition, a missingness indicator matrix $\mathbf{R}$ is constructed for $\mathbf{D}$, allowing us to later distinguish between $\mathbf{D}_{\text{mis}}$ and $\mathbf{D}_{\text{obs}}$, and all elements of $\mathbf{D}_{\text{mis}}$ are set to 0. A DA is then initialized according to the dimensions of $\mathbf{D}$; the default architecture is a three-layer network with 256 nodes per layer.

In the training stage, the following five steps are repeated (see Figure 2 for a visual schematic and Online Appendix 2B for a more formal description): (1) $\mathbf{D}$ and $\mathbf{R}$ are shuffled and sliced row-wise into paired mini-batches ($\mathcal{B}_1, \mathcal{B}_2, ..., \mathcal{B}_n$) to accelerate convergence; (2) mini-batch inputs are partially corrupted through multiplication by a Bernoulli vector $\mathbf{v}$ (default $p = 0.8$); (3) in line with standard implementations of dropout, outputs from

half of the nodes in hidden layers are corrupted using the same procedure; (4) a forward pass through the DA is conducted and the reconstruction error on predictions of $\tilde{\mathbf{x}}_{\text{obs}}$ is calculated using the loss functions defined in Equation 7; and (5) loss values are aggregated into a single term and backpropagated through the DA, with the resulting error gradients used to adjust weights for the next epoch.

Finally, once training is complete, the whole of $\mathbf{D}$ is passed into the DA, which attempts to reconstruct all (i.e., originally observed *and* originally missing) corrupted values. A completed dataset is then constructed by replacing $\mathbf{D}_{\text{mis}}$ with predictions of the originally missing values from the network's output. This stage is repeated M times.

3 Accuracy Tests

How does MIDAS perform in practice? The next two sections present tests of the method's accuracy and scalability involving both simulated and real data. We begin with two tough simulation tests that gauge MIDAS's accuracy under the multivariate normal conditions assumed by the dominant approach to MI (without building a linearity constraint into the MIDAS model). The first is the "MAR-1" experiment first conducted by King et al. (2001), which assesses whether MIDAS generates correct estimates of linear regression parameters; the second is the continuous component of a more general test conducted by Kropko et al. (2014), which also assesses the accuracy of MIDAS's imputed values. The third part of the section tests MIDAS's performance on similar metrics in a more realistic context by simulating a variety of missingness conditions in a popular census dataset.

Figure 3. Estimated Posterior Densities in MAR-1 Simulation Experiment

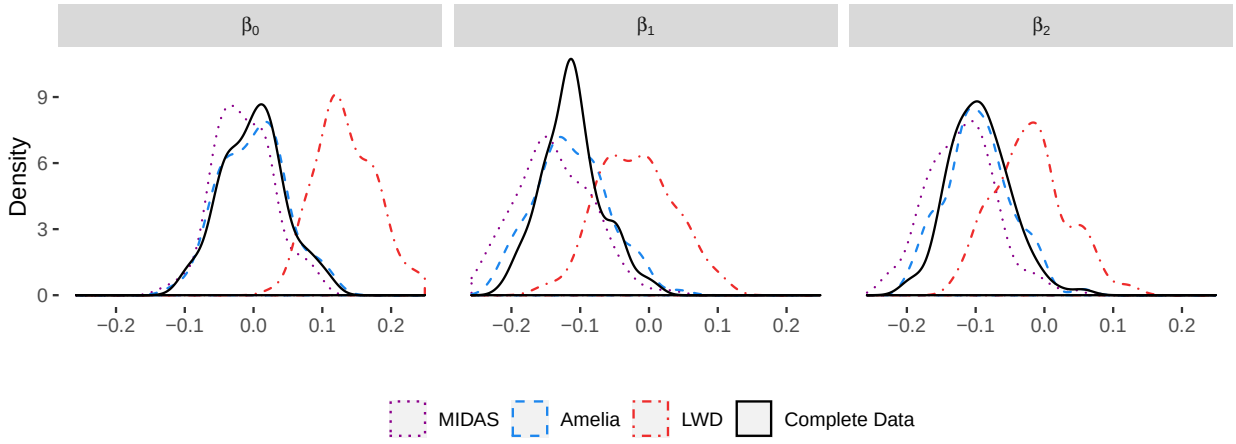

Coefficient estimates from a linear regression based on Monte Carlo-simulated data with 500 rows, 72% of which are fully observed, and five standardized variables drawn from a multivariate normal distribution.

3.1 MAR-1 Experiment

The MAR-1 experiment involves simulating 100 datasets containing 500 rows and five (moderately correlated) standardized variables $Y, X_1, ..., X_4$ from a multivariate normal distribution. A mixed pattern of missingness is introduced, leaving an average of 72% of rows in each sample fully observed: Y and X_4 are MCAR, while X_1 and X_2 are MAR as a function of X_3. We estimate the linear model $Y = \beta_0 + \beta_1 X_1 + \beta_2 X_2$ using four strategies: (1) MIDAS, which we implement using our `Python` class **MIDASpy**; (2) multivariate normal MI, implemented with the **Amelia** package in `R` (Honaker et al. 2011), which employs an expectation-maximization with bootstrapping algorithm; (3) listwise deletion, and (4) analysis of the complete dataset.[9]

Figure 3 plots the posterior densities of the estimated coefficients on β_0, β_1, and β_2

[9]In all tests conducted in this and the next section, $M = 10$ for all MI algorithms.

for each strategy. For all three parameters, MIDAS yields very similar results to **Amelia**. Both sets of estimates are close to the true density, though in the case of β_1 have smaller peaks and larger variances (due to their lower information content). Listwise deletion estimates, by contrast, are severely biased away the true density of every parameter, mostly possessing the incorrect sign as well as a higher variance than the other densities. In Online Appendix 3, we further demonstrate that MIDAS and *Amelia* produce accurate estimated 95% confidence intervals, with listwise deletion again performing substantially worse.

3.2 Simulation Test of Imputation and Linear Model Quality

The continuous portion of Kropko et al.'s (2014) simulation-based accuracy test involves generating 1,000 multivariate normal datasets with 1,000 rows and eight standardized variables, and inducing MAR missingness in five of the latter (with proportions of 0.1, 0.1, 0.1, 0.1, and 0.25). To assess how the strength of relationships between variables affects MIDAS's performance, we generate two versions of the simulated datasets: one in which correlations between variables are moderate and another in which they are strong.[10]

In addition to MIDAS, five missing-data strategies are applied to the incomplete datasets: (1) conditional MI, implemented with the **mi** package in `R` (Su et al. 2011); multivariate normal MI, implemented with (2) **Amelia** and (3) the **norm** package in `R` (which employs a traditional expectation-maximization algorithm) (Schafer and Olsen 1998); (4) listwise

[10] As Kropko et al. use the random data function *rdata.frame* in `R` to simulate the datasets, we model moderate and strong intercorrelations by setting the `eta` argument of this function to 300 and to 1000, respectively.

Figure 4. Inverse Imputation and Linear Model Accuracy in Kropko et al. Simulation Test

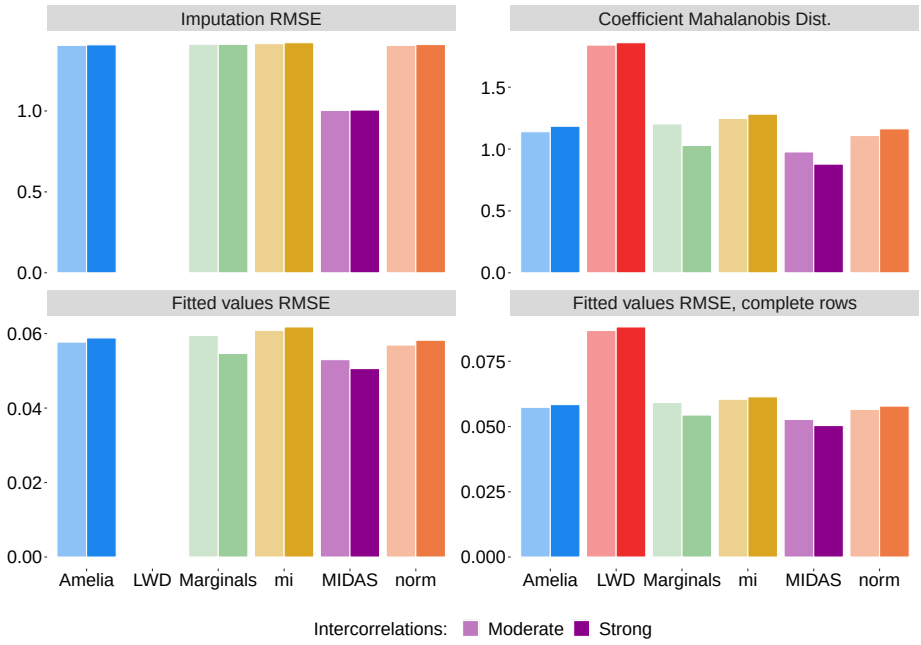

The results are based on Monte Carlo-simulated data with 1,000 rows and eight standardized variables, five of which contain MAR missingness, drawn from a multivariate normal distribution. Lower RMSE indicates greater imputation/fitted-value accuracy; lower Mahalanobis distances indicate greater coefficient accuracy.

deletion; and (5) replacing missing values with draws from each variable's marginal distribution. The six strategies are assessed on two metrics: (1) RMSE relative to true values (averaging imputed values); and (2) the accuracy of coefficient estimates from a regression of one variable on the remaining seven, measured as (i) the Mahalanobis distance between model estimates and complete-data estimates, (ii) the RMSE of model fitted values relative to complete-data fitted values, and (iii) the previous metric excluding incomplete rows.

The results are displayed in Figure 4. In the moderate-correlation scenario, MIDAS outperforms the other four MI strategies on all four metrics. When we strengthen correlations, this gap remains essentially the same in terms of imputation accuracy but becomes even

larger in terms of coefficient and fitted-value accuracy (except with respect to marginal draws). Even without a linearity constraint, therefore, MIDAS can produce accurate imputations and parameter estimates under multivariate normality, with its absolute and relative performance improving with the strength of relationships between variables.

3.3 Applied Test with Adult Dataset

Real data, of course, are rarely multivariate normal. We thus supplement the previous simulation exercises with an applied accuracy test based on the Adult dataset, an extract from the 1994 United States Census that measures 15 characteristics of 48,842 individuals (a mixture of continuous and categorical variables).[11] We select this dataset for two reasons. First, in addition to being frequently used by social scientists, it is a standard benchmarking dataset for machine learning tasks. Second, it is one of the few real social science datasets we were able to find that is almost entirely complete — just 0.009% of values are missing — which gives us near-complete discretion to manipulate missingness in the test (while mitigating possible concerns about the exclusion of originally missing values). Summary statistics for the dataset are provided in Online Appendix 3.

In contrast to the previous tests, we separately induce varying proportions of MCAR, MAR, and MNAR missingness in the dataset. For each missingness pattern, we create

[11] Kropko et al. (2014) also conduct an applied test involving the American National Election Studies (ANES) dataset. In Online Appendix 4, we incorporate MIDAS into the imputation accuracy component of this test, again finding that it produces more accurate imputed values than other MI algorithms for all variables.

Figure 5. Results of Applied Imputation Accuracy Test

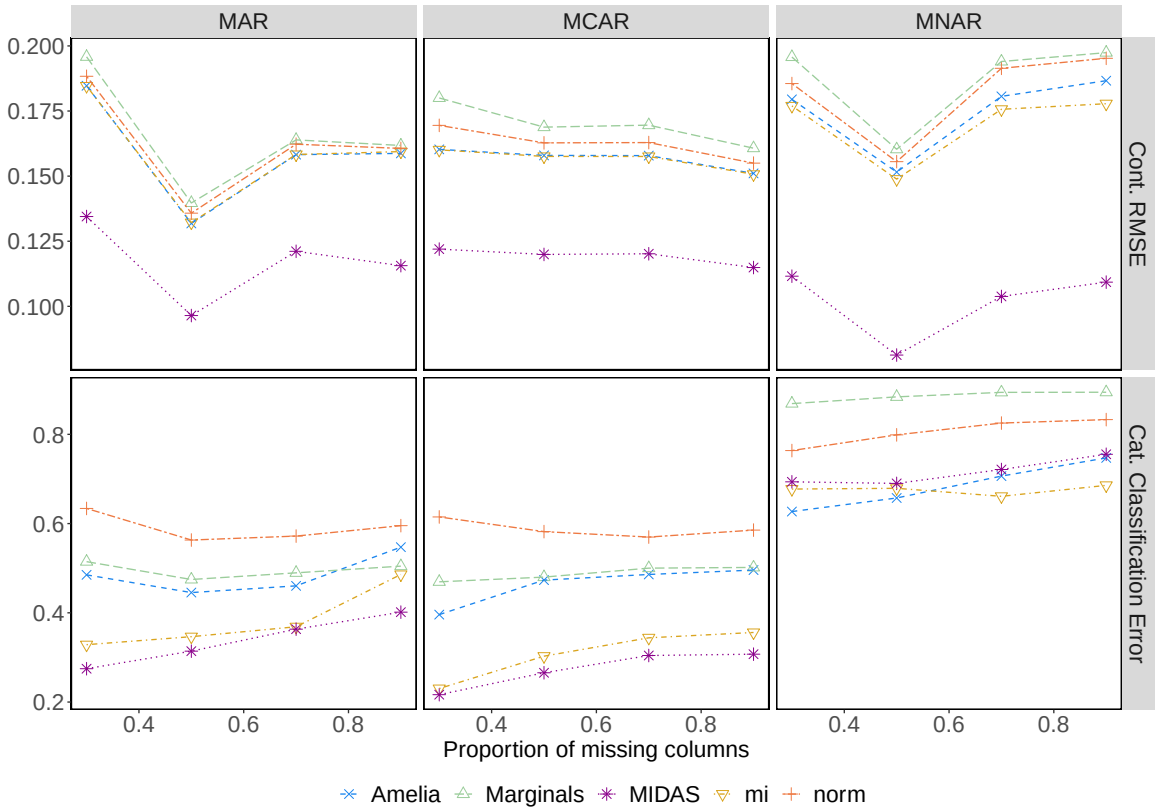

MCAR, MAR, and MNAR missingness are separately induced in varying proportions of randomly selected columns in the Adult dataset, with up to 50% of values are set as missing. Lower RMSE and classification error values indicate greater imputation accuracy.

four versions of the dataset in which 30%, 50%, 70%, and 90% of columns are randomly selected for corruption. In the MCAR treatment, half of the values in the selected columns are randomly set to missing. In the MAR treatment, a missingness indicator L is randomly drawn from the non-selected columns. If L is continuous, a subset of observations at or below its median value are set to missing in the selected columns; if L is categorical, half of its categories are randomly sampled and a subset of corresponding observations in the selected columns are set to missing. The MNAR treatment is similar to the MAR treatment, with the key difference that L is the selected column *itself*. These treatments are described

in more detail in Online Appendix 3. Since **Amelia**'s runtime substantially increases when categorical variables have more than 10 classes (which is prohibited in its default settings), $native\_country$, $occupation$, and $education$ are excluded from the corruption process.

We include the same five missing-data strategies as the previous test, comparing their imputation accuracy using similar metrics: the RMSE of imputed versus actual values for continuous variables; and classification error for categorical variables. We refrain from conducting a model-based accuracy test because, unlike in Kropko et al.'s simulation, we do not know the true joint distribution of the data. We instantiate MIDAS with two hidden layers of 256 nodes, an input corruption proportion of 0.75, and 20 training epochs, leaving all other hyperparameters at their default settings. **Amelia** only converges with a ridge prior of 1% of the number of rows in the imputation model, a modification that shrinks covariances between variables and thus introduces some degree of bias (Honaker et al. 2011, 19-20). We swap the earlier version of the **norm** package, which is unable to handle the treated datasets, with an updated version based on the same algorithmic logic (Novo 2015). To enable **mi** to complete the test in a reasonable time, we modify its settings to complete datasets after either 15 imputation iterations (default = 30) or the default maximum iteration time of 20 minutes — whichever comes first.

The results are summarized in Figure 5. Across almost all corruption levels and missingness patterns, MIDAS's imputed values are more accurate than those of other strategies. This advantage is largest for continuous variables: the mean RMSE of MIDAS imputations is around 30% lower than that of the next best algorithm, **mi**. The gap in classification

accuracy is narrower but still clear in the MAR and MCAR scenarios. Under MNAR, **Amelia** and **mi** are the best category classifiers, though MIDAS's performance is comparable. In short, as we move to a more realistic setting in which multivariate normality does not hold, MIDAS continues to exhibit strong relative performance on key metrics of accuracy.

4 Scalability Tests

To facilitate comparison, the previous tests were conducted on small or medium-sized datasets that do not pose (major) computational problems for existing MI algorithms. We now relax this constraint, comparing the algorithms' efficiency in handling progressively larger datasets. We conduct separate tests for increasing numbers of columns and rows, though place greater weight on the former: additional columns are more computationally demanding for MI algorithms than additional rows because they entail a greater marginal increase in the number and complexity of relationships within the observed data.[12]

4.1 Column-Wise Scalability

Rather than scaling up a purely simulated dataset, which is unlikely to capture the complexity and richness of real data, we conduct both tests using the 2018 Cooperative Congressional Election Study (CCES), a large-scale electoral survey commonly used by political scientists that encompasses a representative sample of 60,000 respondents in the United

[12]Given the computational demands of these tests, we conducted them on an Amazon Web Services Linux m5.xlarge EC2 Instance virtual server (16 GB RAM, 4 vCPUs) running Ubuntu 18.04.

States. We focus on the subset of personal profile questions asked to all respondents, in addition to a selection of voting- and political activity-related questions (details are provided in Online Appendix 5). To generate a baseline sample for the column-wise test, we remove all columns that are perfectly collinear or that contain at least 10,000 missing values (which generally indicates structural missingness associated with survey flow) and all rows with responses of "don't know." This leaves a sample of 30,421 rows and 144 variables. Once categorical variables are one-hot encoded, there are 443 "effective" columns.

To examine the effect of increasing dataset width on imputation speed, we randomly draw columns without replacement from the baseline sample based on a target number of effective columns, which we vary from 25 to 400. If, after selecting a given variable, the number of effective columns is more than 25% higher than the target, this variable is replaced and a new one is selected. After each dataset has been generated, we induce 50% MCAR missingness in every column. To ensure that the data do not become too sparse for imputation, we include the fully observed $gender$ and $birthyr$ variables in all samples.

We test the same five MI strategies as before, comparing the time they take to complete 10 datasets. MIDAS is instantiated with three 256-node layers, a dropout rate of 0.75, and 30 training epochs — a conservative setup, especially for narrow datasets. Where possible, we parallelize other MI algorithms using the **doparallel** and **foreach** packages in `R`.

Figure 6 displays the results, including predicted values from a regression of runtime on the effective number of columns (which includes quadratic terms for **Amelia** and **norm** due to the distribution of their runtimes). Differences in scalability emerge even at the smallest

Figure 6. Results of Column-Wise Scalability Test

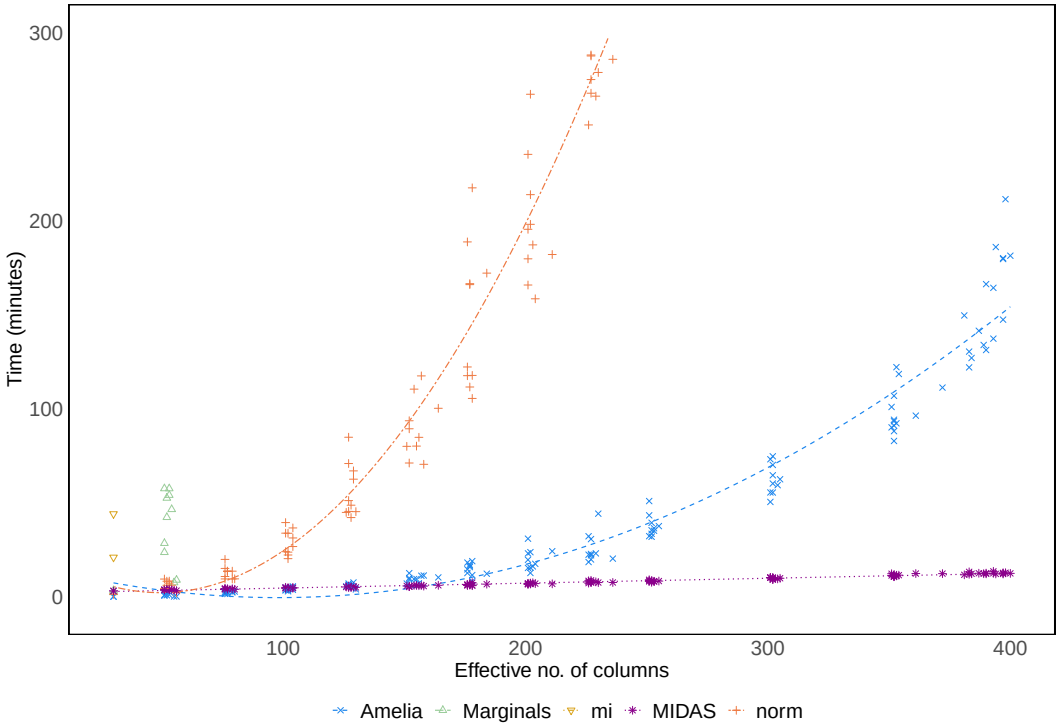

The *y*-axis measures the time taken to produce 10 completed versions of a CCES sample with 50 percent MCAR missingness; the *x*-axis measures the number of columns in the sample after categorical variables have been one-hot encoded. Dashed lines show predicted values from a regression of *y* on *x* (including quadratic terms for **Amelia** and **norm**).

widths, with the **mi** package and marginal draws recording runtimes several times longer than the remaining three algorithms for samples with 50 columns.[13] The latter routines perform similarly up to this width, with **Amelia** slightly faster than **Norm** and MIDAS but (unlike other algorithms) failing to converge on several occasions. Note again that we do not adjust the MIDAS network's size by width; a three-layer, 256-node network is not necessary for narrow datasets, and a leaner architecture would result in faster computation.

As the number of columns increases, MIDAS's efficiency emerges clearly. MIDAS be-

[13]We therefore drop these two strategies for higher numbers of columns.

comes faster than **norm** at a width of around 75 columns and **Amelia** just before 125 columns. By 200 columns, MIDAS is three times quicker than **Amelia** and almost 30 times quicker than **norm**. At the maximum number of columns in the test, 400, MIDAS is 12 times faster than **Amelia**. Extrapolating from these results, **Amelia** would take more than 6,000 hours to produce 10 completed versions of the full CCES, approximately 100 times longer than MIDAS. As indicated by the slope of the regression lines, MIDAS's efficiency advantage increases exponentially with the effective number of columns: the relationship between computation time and data width is linear for MIDAS but quadratic for **Amelia** and the other algorithms. This constitutes a major advantage in the Big Data era, in which datasets can contain thousands or even tens of thousands of variables.

4.2 Row-Wise Scalability

We test row-wise scalability by extracting a similar baseline sample from the CCES. To ensure a comparable overall runtime to the column-wise test, we focus on personal profile variables that are continuous, binary, or nominal and have fewer than seven levels. In total, the sample contains 22 variables and 34,441 complete rows. We vary sample length by bootstrapping rows to create datasets with between 5,000 and 500,000 rows. We then induce MCAR missingness in 30% of values in each column. As in the column-wise test, we exclude $birthyr$ and $gender$ from the missingness treatment to prevent excessive sparsity. As the baseline sample is smaller and less complex than before, we shrink the MIDAS network to two layers of 256 nodes and set the number of training epochs as 20.

Figure 7. Results of Row-Wise Scalability Test

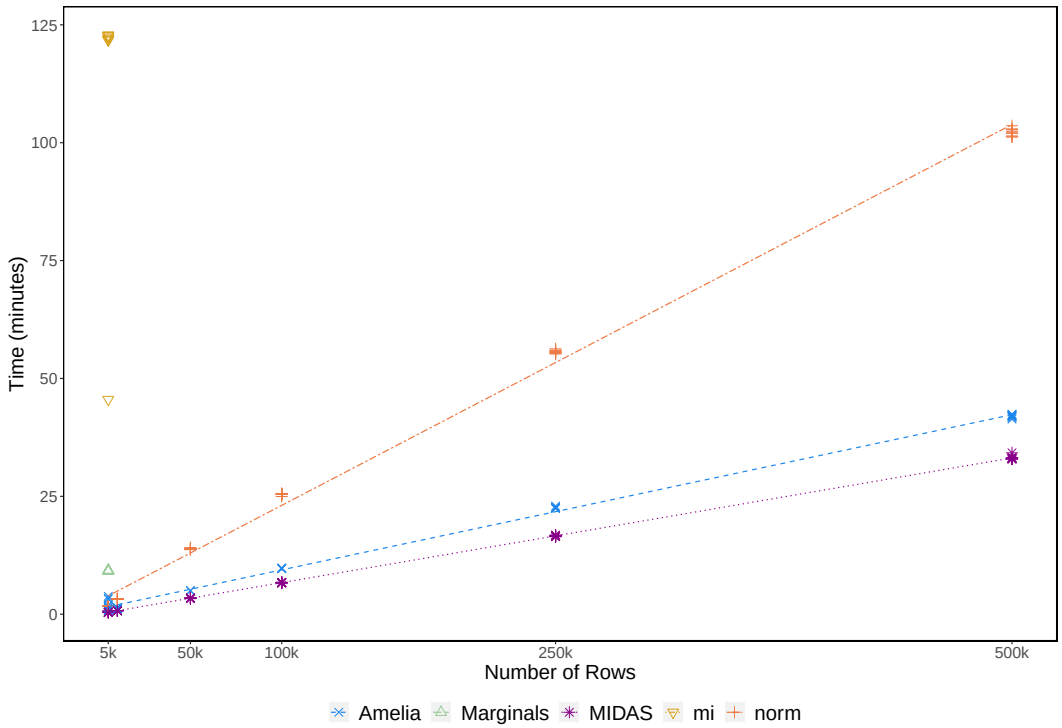

The *y*-axis measures the time taken to produce 10 completed versions of a CCES sample with 30 percent MCAR missingness; the *x*-axis measures the number of rows in the sample. Dashed lines show regression-based predicted values for each strategy.

The results are plotted in Figure 7. Across all sample lengths, MIDAS is the most efficient strategy. For datasets with 500,000 rows, MIDAS's average runtime is three times quicker than than that of **norm**, the third fastest algorithm, and 25 percent quicker than that of **Amelia**, the second fastest, with these gaps increasing in proportion to length. Unlike in the column-wise test, therefore, computation time scales linearly with the number of rows for MIDAS as well as **norm** and **Amelia**, a finding consistent with the less intensive computational demands created by additional rows. As before, **mi** and marginal draws record the longest runtimes, producing the completed datasets in an average of 115

minutes and 9.2 minutes, respectively, at the smallest number of rows (5000).[14]

Note that while the performance gap between MIDAS and **Amelia** is smaller in this test, there are caveats to the latter's results. **Amelia** did not converge with any dataset without the inclusion of a bias-inducing ridge prior in the imputation model (of 0.005 times the number of rows), most likely due to high correlations among some variables. Even with this modification, it failed to converge in 16 of the 60 iterations of the simulation.

5 Applied Illustration: Estimating Ideology from CCES Data

In this section, we provide a brief illustration of MIDAS's capacity to handle real missing-data situations whose scale presents difficulties for existing MI algorithms. We continue to focus on the CCES, whose large number of columns — a feature shared with other electoral surveys — can prevent the usage of such algorithms. Specifically, we use MIDAS to shed new light on the distribution of political ideology among respondents, a topic of substantive interest to scholars of electoral politics in the United States and elsewhere.

Respondents to the CCES are asked to report their ideological position on a seven-point scale ranging from 1 for "Very Liberal" to 7 for "Very Conservative." Self-reported ideology, however, is known to be a noisy proxy for underlying beliefs (for instance, due to social desirability biases and variation in ideological positions across policy dimensions). A variety of approaches have been proposed to capture respondents' latent ideology, most of which involve estimating ideology using responses to policy-related questions. In the 2018

[14]We again exclude these two strategies for longer samples.

CCES, individuals are asked their opinion on a series of policy proposals in areas such as the budget, healthcare, and environmental protection. These items have a higher rate of nonresponse than the CCES in general, with an average of 14% of respondents failing to provide an answer. Does this missingness affect estimates of latent ideology?

Building on recent work by Ramseyer and Rasmussen (2016), we regress respondent i's self-reported ideology on responses to 19 policy questions in the CCES (see Online Appendix 6A for the list):

$$\text{Self-Reported Ideology}_i = \alpha + \sum_{j=1}^{19} \beta_j \times \text{Policy}_{i,j} + \epsilon_i \tag{8}$$

where j denotes a given policy question. The fitted values from Equation 8 represent estimates of latent ideology. We compare such estimates under two missing-data strategies: (1) listwise deletion (following Ramseyer and Rasmussen); and (2) MIDAS, which we implement using a rich battery of 163 demographic and socioeconomic variables — an imputation model too large to be computed by any existing MI algorithm — and a two-layer, 256-node network trained for 200 epochs.[15] MIDAS allows us to produce estimates for more than 10,000 more respondents, almost one-fifth of the full CCES.

Figure 8 plots the densities of the two sets of latent ideology estimates. The two distributions have similar variances but divergent peaks; the null hypothesis that they are

[15]Some existing MI algorithms, such as **Amelia**, can accommodate subsets of the MIDAS imputation model. These subsets, however, tend to exclude strong predictors of missingness in the policy items. Consequently, as shown in Online Appendix 6B, the resulting latent ideology estimates are substantially closer to those produced by listwise deletion.

Figure 8. Regression-Based Estimates of CCES Respondents' Latent Ideology

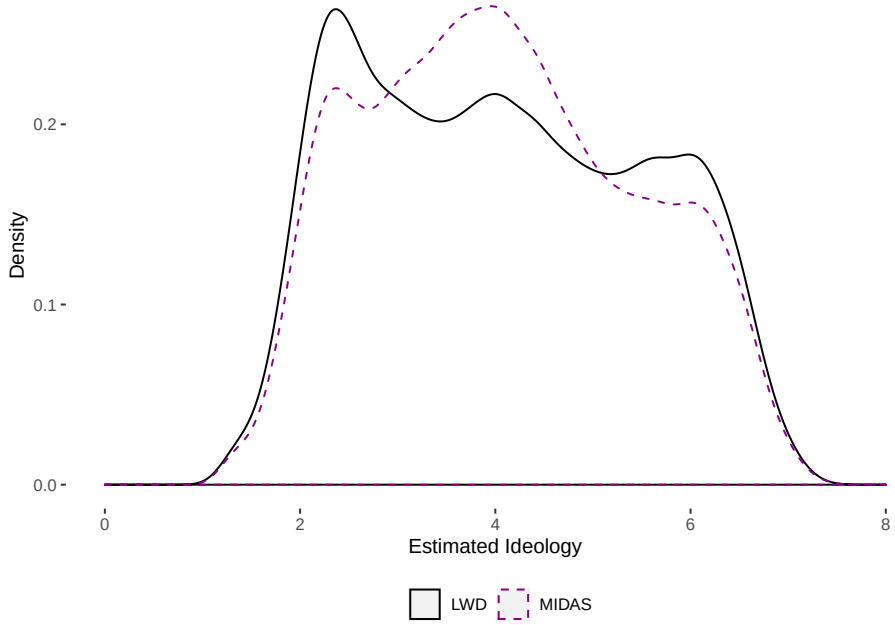

drawn from the same distribution can be rejected under a Kolmogorov-Smirnov test. The distribution of listwise deletion estimates is skewed toward the left (liberal) side of the ideology scale — the modal estimate is 2 — though also contains smaller peaks in the center and on the right (conservative) side. The MIDAS estimates, in contrast, follow a more normal shape, peaking at 4. In the absence of MI, therefore, there is a danger that analysts could overestimate the proportion of strong liberal and strong conservative respondents.

This finding also has implications for our understanding of the relationship between ideology and other variables of substantive interest in the CCES, such as respondents' assessment of President Donald Trump's performance in office. Table 1 shows the results of regressing responses to the CCES presidential job approval question, which range from 1 for "strongly approve" to 4 for "strongly disapprove," on (1) self-reported ideology and (2)

Table 1. Regression of Presidential Job Approval on Different Measures of Ideology

Measure of Ideology	β	Std. Error	Adj. R^2	N
Self-reported	-0.475	0.002	0.506	48713
Regression-based (MIDAS)	-0.697	0.002	0.616	60000

the MIDAS-based regression estimates of latent ideology.[16] In both models, the estimated coefficient on the ideology measure is negative and statistically significant, indicating that respondents classified as more liberal express lower average levels of presidential job approval. The MIDAS-based measure, however, is a far better predictor of job approval than the self-reported alternative, possessing a coefficient almost 50% larger (with an identical standard error) and accounting for 20% more model-adjusted variance in the outcome.

6 Potential Limitations

While MIDAS's flexibility render it suitable for a wide range of missing-data problems, there are nevertheless circumstances in which it may perform suboptimally. First, MIDAS cannot, of course, avoid bias when the usual assumptions of MI are violated: data are MNAR, the posited distribution of the data is a poor approximation to reality, or the imputation model is misspecified in some other way. However, as noted earlier — and demonstrated in the applied accuracy test — MIDAS can still perform relatively well under MNAR when there are strong predictors of missingness in the imputation model.

Second, like other approaches to MI, MIDAS is not guaranteed to perform well with cer-

[16]We remove "not sure" responses from the job approval variable for the self-reported model. These values are imputed in the MIDAS model.

tain unconventional data structures, such as non-exchangable data, multilevel data, and spatially lagged data. In general, however, we have found MIDAS to be surprisingly effective at learning observed-data relationships within these structures (without including any special features in the imputation model). Online Appendix 7 provides an illustration of this capacity in the context of time-series cross-sectional data — perhaps the most common form of non-exchangable data in social science research — adapting an exercise conducted by Honaker and King (2010) to show how MIDAS can impute smooth nonlinear time trends in economic variables. This illustration, which involves another dataset too large to be processed by existing MI algorithms, highlights how the flexibility of neural networks can sometimes mitigate the need for manual feature transformation.

Finally, MIDAS inherits the general risks associated with neural network-based methods. These include misspecification of hyperparameters, which can result in bias; overfitting — despite MIDAS's heavy inbuilt regularization — the likelihood of which increases with the size, dimensionality, and sparsity of the dataset; and poor performance on very small datasets. Such risks can be compounded by the "black box" nature of neural networks, which makes it difficult for analysts to conduct parameter and posterior checks to identify problems. Our software for implementing MIDAS offers two diagnostic tools to help analysts conduct such checks (see Online Appendix 1 for details): (1) the technique of "overimputation" (Honaker et al. 2011, 27-29), which involves sequentially removing observed values and checking the accuracy of their imputations; and (2) the use of a variational autoencoder component to generate an alternative set of imputations based on more

stringent assumptions about the distribution of the latent input space. We acknowledge, however, that these tools do not guarantee detection of all problems.

7 Concluding Remarks

As the scale and complexity of real-world data continue to grow, it is increasingly important that analysts have access to accurate, fast, and scalable methods for analyzing missing values. The approach to MI we have developed in this article, MIDAS, seeks to deliver these advantages by drawing on recent theoretical and computational advances in deep learning. A battery of tests involving real and simulated data suggest that MIDAS can provide gains in accuracy over existing approaches to MI (as well as listwise deletion) even in small- and medium-sized applications, with larger improvements when data possess more complex features. Relative to leading MI algorithms, it can offer improvements in efficiency when datasets contain as few as 200 columns (with the gap increasing exponentially beyond this width) and 5,000 rows (with the gap increasing linearly beyond this length).

To be sure, MIDAS is not a panacea for missing-data problems in the emerging era of Big Data. As discussed earlier, despite its flexibility, the approach is not guaranteed to perform well with every type of data and may be not be straightforward to optimize for particular applications. Nevertheless, we believe that it constitutes a helpful addition to the methodological toolkit of analysts and nicely complements the strengths of existing approaches to MI. Indeed, it is precisely the kinds of applications with which these approaches can struggle where MIDAS comes into its own.

Acknowledgments

For valuable feedback on previous drafts, we are grateful to Matthew Blackwell, Andrew Eggers, Jeff Gill, Kosuke Imai, Gary King, Walter Mattli, Alex Stenlake, and the anonymous reviewers of *Political Analysis*. We also thank Kin Wai Chan, James Honaker, Musashi Jacobs-Harukawa, Ankur Moitra, and Devrarat Shah for helpful conversations on this research and Jonathan Kropko for generously sharing replication code. Earlier versions of this article were presented at the Quantitative Social Science Colloquium at Princeton University and the Artificial Intelligence and Machine Learning Society at the University of Queensland. The software accompanying this article was developed by Ranjit Lall, Thomas Robinson, and Alex Stenlake.

Data Availability Statement

Replication materials for this article are available in Lall and Robinson (2020).

References

Beaulieu-Jones, B. K. and C. Greene (2016). Semi-supervised learning of the electronic health record for phenotype stratification. *Journal of Biomedical Informatics 64 (2)*, 168–178.

Cranmer, S. J. and J. Gill (2013). We have to be discrete about this: A non-parametric imputation technique for missing categorical data. *British Journal of Political Science 43 (2)*, 425–449.

Duan, Y., Y. Lv, W. Kang, and Y. Zhao (2014). A deep learning based approach for traffic data imputation. In *17th International IEEE Conference on Intelligent Transportation Systems (ITSC)*, pp. 912–917. IEEE.

Gal, Y. and Z. Ghahramani (2016). Dropout as a bayesian approximation: Representing model uncertainty in deep learning. In *Proceedings of the 33rd International Conference on Machine Learning*, pp. 1050–1059. ACM.

Gondara, L. and K. Wang (2018). Mida: Multiple imputation using denoising autoencoders. In *Pacific-Asia Conference on Knowledge Discovery and Data Mining: Advances in Knowledge Discovery and Data Mining*, pp. 260–272. Springer, Cham.

Hinton, G. E., N. Srivastava, A. Krizhevsky, I. Sutskever, and R. R. Salakhutdinov (2012). Improving neural networks by preventing co-adaptation of feature detectors. *Neural Networks 2*, 1–18.

Honaker, J. and G. King (2010). What to do about missing values in time-series cross-section data. *American Journal of Political Science 54 (2)*, 561–581.

Honaker, J., G. King, and M. Blackwell (2011). Amelia II: A program for missing data. *Journal of Statistical Software 45 (7)*, 1–47.

King, G., J. Honaker, A. Joseph, and K. Scheve (2001). Analyzing incomplete political science data: An alternative algorithm for multiple imputation. *American Political Science Review 95 (1)*, 49–69.

Kropko, J., B. Goodrich, A. Gelman, and J. Hill (2014). Multiple imputation for continuous and categorical data: Comparing joint multivariate normal and conditional approaches. *Political Analysis 22 (4)*, 497–219.

Lall, R. (2016). How multiple imputation makes a difference. *Political Analysis 24 (4)*, 414–433.

Lall, R. and T. Robinson (2020). Replication Data for: The MIDAS Touch: Accurate and Scalable Missing-Data Imputation with Deep Learning. https://doi.org/10.7910/DVN/UPL4TT, Harvard Dataverse, V1.

Little, R. J. and D. Rubin (1987). *Statistical Analysis with Missing Data*. New York, NY: Wiley.

Novo, A. A. (2015). *norm*. Vienna, Austria: R Foundation for Statistical Computing.

Ramseyer, J. M. and E. B. Rasmussen (2016). Voter ideology: Regression measurement of position on the left-right spectrum. Working paper.

Rubin, D. B. (1987). *Multiple Imputation for Nonresponse in Surveys*. New York, NY: John Wiley & Sons.

Schafer, J. L. and M. K. Olsen (1998). Multiple imputation for multivariate missing-data problems: A data analyst's perspective. *Multivariate Behavioral Research 33 (4)*, 545–571.

Su, Y.-S., A. Gelman, J. Hill, and M. Yajima (2011). Multiple imputation with diagnostics (mi) in r: Opening windows into the black box. *Journal of Statistical Software 45 (2)*, 1–31.

van Buuren, S. (2012). *Flexible Imputation of Missing Data*. Boca Raton, FL: Taylor and Francis.

Vincent, P., H. Larochelle, Y. Bengio, and P.-A. Manzagol (2008). Extracting and composing robust features with denoising autoencoders. In *Proceedings of the 25th International Conference on Machine Learning*, pp. 1096–1103. ACM.

Online Appendices for "The MIDAS Touch: Accurate and Scalable Missing-Data Imputation with Deep Learning"

Ranjit Lall* Thomas Robinson†

January 14, 2021

Contents

*London School of Economics and Political Science. Email: r.lall@lse.ac.uk.
†Durham University. Email: thomas.robinson@durham.ac.uk.

1 Summary of Diagnostic Tools

The performance of modern machine learning techniques depends heavily on the length of training — which affects the risk of overfitting — and the choice of model hyperparameters (Probst et al. 2019). To help users of MIDAS assess the fit of the imputation model and calibrate hyperparameters, we provide two diagnostic tools. The first is the technique of "overimputation" (Blackwell et al. 2017; Honaker et al. 2011). This involves sequentially removing observed values from the dataset, generating a large number of imputations for each value, and checking the accuracy of these imputations. Accuracy is measured with (1) the RMSE of imputed values versus true values for continuous variables and (2) classification error for categorical variables. To ensure a good fit, we recommend selecting the number of training epochs that minimizes the average value of these metrics (weighted by the proportion of continuous versus categorical variables). By reducing the risk of overtraining, this "early stopping" rule effectively serves as an extra layer of regularization in a MIDAS network.

In the **MIDASpy** class, overimputation can be implemented using the `overimpute` function (described in more detail on the MIDAS GitHub page). This function plots values of the RMSE and classification error metrics for each training epoch. Initially, these values should decline with additional epochs as the MIDAS network learns increasingly accurate approximations of the missing-data posterior. As suggested above, if and when error begins to rise, the number of epochs specified in the `train.model` function should be capped before this point. The `plot_all` argument of `overimpute` compares the distribution of overimputed versus original values, allowing users to visually inspect whether the former fall within a reasonable range (implying a good model fit). The default hyperparameter settings for `overimpute` are a corruption proportion (`spikein`) of 0.1 and 100 training epochs (`training_epochs`).

The second diagnostic tool is the generation of entirely new observations using a variational autoencoder component. Variational autoencoders are another extension of the classical autoencoder that encode inputs not to a fixed vector $\mathbf{z}$ but to a *distribution* over the latent space $p(\mathbf{z})$ (Kingma and Welling 2013; Rezende et al. 2014). The loss function minimized during training includes a regularization term (in addition to the usual reconstruction term) that constrains the latent distribution to approximate normality, reducing the risk of an irregular latent space in which similar data points can become very different after decoding. Samples from the latent distribution $\mathbf{z} \sim p(\mathbf{z}|\mathbf{x})$ will thus tend to more closely follow the input density than a regular (deterministic) latent representation $\mathbf{z}$, rendering them better suited to the task of generative modeling.

In the **MIDASpy** class, the variational autoencoder component can be activated by setting `vae_layer = True` in the `Midas` function. This inserts a variational autoencoder layer after the denoising portion of a MIDAS network, which probabilistically maps inputs to a latent distribution in the manner described above. After training, samples are drawn from this distribution and decoded to produce new observations. In general, the greater the similarity between these observations and the input data, the better the fit of the imputation model. Default settings for `vae_layer` hyperparameters — which include the number of normal clusters assumed to characterize the input data (`latent_space_size`), the variance of these distributions (`vae_sample_var`), and the strength of our normal prior (`vae_alpha`) — follow standard conventions in autoencoder applications.

We favor overimputation and data generation over customary train/test split approaches to model validation for two reasons. First, the latter have been found to systematically underestimate error in autoencoders and other unsupervised methods of nonlinear dimensionality reduction where there is no clear target value (Christiansen 2005; Scholz 2012). Second, they prevent us from training the MIDAS network on the full dataset, which impedes accuracy — and could seriously compromise performance at high levels of

missingness.

2 Technical Details on MIDAS Model and Algorithm

2A Objective Function

This section offers additional technical details on the MIDAS model's objective function. Recall from the main text that a traditional autoencoder first maps an input vector $\mathbf{x}$ to a lower-dimensional representation $\mathbf{y}$ via a deterministic series of transformations $\mathbf{y} = f_\theta(\mathbf{x})$, parameterized by $\theta = \{\mathbf{W}, \mathbf{b}\}$ (Equation 3), and then maps this representation back to a reconstructed vector $\mathbf{z}$ via a converse series of transformations $\mathbf{z} = g_{\theta'}(\mathbf{y})$, parameterized by $\theta' = \{\mathbf{W}', \mathbf{b}'\}$ (Equation 4). Each element i of the input vector $\mathbf{x}_i$ is thus mapped to a corresponding element of the hidden representation $\mathbf{y}_i$ and the reconstruction $\mathbf{z}_i$. The parameters of this model are trained to minimize the average reconstruction error:

$$\theta^*, \theta'^* = \underset{\theta^*, \theta'^*}{\arg\min} \frac{1}{N} \sum_{i=1}^{N} L(\mathbf{x}_i, \mathbf{z}_i) \tag{A1}$$

$$= \underset{\theta^*, \theta'^*}{\arg\min} \frac{1}{N} \sum_{i=1}^{N} L(\mathbf{x}_i, g_{\theta'}(f_\theta(\mathbf{x}_i))) \tag{A2}$$

where L is a loss function (such as a mean squared error function).

In a denoising autoencoder, we again optimize these parameters to minimize the average reconstruction error. Unlike before, however, $\mathbf{z}$ is a deterministic function of $\tilde{\mathbf{x}}$, the corrupted input, instead of $\mathbf{x}$. In a MIDAS model, we only seek to minimize the reconstruction error on corrupted values that were originally observed. That is, we want $\mathbf{z}$ to be as close as possible to $\tilde{x}_{\text{obs}}$ (we do not know the original values of $\tilde{x}_{\text{mis}}$). If $\mathbf{D}$ consists of two random variables X and Y with joint probability distribution $p(X, Y)$, the overall

joint distribution can be characterized as:

$$q^0(X, \tilde{X}_{\text{obs}}, \tilde{X}_{\text{mis}}, Y) = q^0(X) q_D(\tilde{X}_{\text{obs}}, \tilde{X}_{\text{mis}}|X) \delta_{f_\theta(\tilde{X}_{\text{obs}}, \tilde{X}_{\text{mis}})}(Y) \tag{A3}$$

where $q^0(X, \tilde{X}, Y)$ is parameterized by $\theta = \{\boldsymbol{\Omega}, \boldsymbol{\psi}\}$. This implies that Y is a deterministic function of both $\tilde{X}_{\text{obs}}$ and $\tilde{X}_{\text{mis}}$. However, the objective function minimized by stochastic gradient descent only includes the former:

$$\underset{\theta^*, \theta'^*}{\arg\min}\, \mathbb{E}_{q^0}(X, \tilde{X}_{\text{mis}})[L(X, g_{\theta'}, (f_\theta(\tilde{X}_{\text{obs}})))] \tag{A4}$$

The implication of this result is that the MIDAS model minimizes the expected loss over the empirical distribution of not only the observed data but also the subset of corrupted data that were originally observed.

2B Training Steps

As discussed in the main text, a MIDAS network is feedforward: given an initial set of weights and biases, data are propagated forward through the hidden layer of the network and aggregate loss is calculated. Weights and biases are then adjusted via the method of backpropagation. Since the MIDAS network is deep (i.e., it contains more than one hidden layer), this adjustment is made sequentially from the last layer to the first. This section provides a more detailed description of the key training steps in the MIDAS algorithm.

Recall that in the pre-training stage, a missingness indicator matrix $\mathbf{D}$ is generated for the input data $\mathbf{D}$, $\mathbf{D}_{\text{mis}}$ is set to 0, and a MIDAS network is parameterized using a variant of Xavier Initialization. In each training epoch, we shuffle and divide $\mathbf{D}$ into B mini-batches $\mathcal{B}_1, \mathcal{B}_2, ..., \mathcal{B}_B$ of size s (default $s = 16$); $\mathbf{R}$ is divided into corresponding mini-batches. This step has the advantage of reducing training time — storing all training data in memory and

calculating loss for the whole sample are memory-intensive, whereas mini-batches can be processed quickly and in parallel — as well as increasing the frequency of model updates, which ensures more robust convergence (for instance, by avoiding local minima).

In the next step, we partially corrupt the input data by multiplying the B mini-batches by a Bernoulli vector $\mathbf{v}$ with $p = 0.8$ (resulting in a corruption rate of 20%):

$$\begin{aligned} \tilde{\mathbf{x}} &= [v^{(0,1)}\mathcal{B}_1, ..., v^{(0,n)}\mathcal{B}_B] \\ \mathbf{v}^{(0)} &\sim \text{Bernoulli}(p = 0.8) \end{aligned} \tag{A5}$$

We then implement dropout regularization by partially corrupting nodes in the hidden layers of the network. This involves multiplying outputs from each layer by another Bernoulli vector with $p = 0.5$ (a corruption rate of 50%):

$$\begin{aligned} \tilde{\mathbf{y}}^{(h)} &= \mathbf{y}^{(h)}\mathbf{v}^{(h)} \\ \mathbf{v}^{(h)} &\sim \text{Bernoulli}(p = 0.5) \end{aligned} \tag{A6}$$

We then perform a full forward pass through the network — using both the corrupted inputs $\tilde{\mathbf{x}}$ and the corrupted hidden nodes $\tilde{\mathbf{y}}^{(h)}$ — to generate our input reconstruction $\mathbf{z}$ (described in Equations 5 and 6 in the main text). Loss is calculated with respect to the subset of corrupted data that were originally observed ($\tilde{\mathbf{x}}_{\mathbf{obs}}$), which is achieved by multiplying the RMSE and cross-entropy loss functions by a missingness indicator vector $\mathbf{r}$ (see Equation 7). A weight decay regularization term λ is included in the calculation to reduce overfitting:

$$E = L(\mathbf{x}, \mathbf{z}, \mathbf{r}) + \lambda||\mathbb{E}[\mathbf{W}]||^2 \tag{A7}$$

In the backpropagation step, we find the gradient of the loss function with respect to the weights of the network.[1] Since the change in error with respect to the weights

[1]For a more in-depth discussion of the backpropagation procedure, see Goodfellow et al. (2016, Chapter 6).

in a given layer ($\mathbf{W}^{(h)}$) depends on the weights in the next layer ($\mathbf{W}^{(h+1)}$), this must be calculated sequentially from the output layer to the input layer. Specifically, for each layer, we must derive $\frac{\partial E}{\partial \mathbf{W}^{(h)}}$. Through two applications of the chain rule, this problem becomes more tractable:

$$\frac{\partial E}{\partial \mathbf{W}^{(h)}} = \frac{\partial E}{\partial \mathbf{y}^{(h)}} \cdot \frac{\partial \mathbf{y}^{(h)}}{\partial \mathbf{W}^{(h)}} \tag{A8}$$

$$= \frac{\partial E}{\partial \mathbf{y}^{(h+1)}} \cdot \frac{\partial \mathbf{y}^{(h+1)}}{\partial \mathbf{y}^{(h)}} \cdot \frac{\partial \mathbf{y}^{(h)}}{\partial \mathbf{W}^{(h)}}, \tag{A9}$$

The first term of Equation A9 indicates that the layer-specific partial derivative of the loss function depends on the derivative with respect to outputs from the next layer. The middle term is the partial derivative of the next layer's outputs with respect to the current layer's, which is equivalent to the derivative of the next layer's activation function $\frac{\partial f(\mathbf{y}^{(h+1)}}{\mathbf{y}^{(h+1)}}$. Since $\mathbf{y}^{(h)}$ is the weighted sum of the inputs into layer h, the right term is simply equal to $\mathbf{y}^{(h-1)}$. Note that the latter two terms are straightforward to derive because the functional form of each layer's activation function is known *a priori*.

Once errors have been fully backpropagated through the network, we use the calculated gradients to update the MIDAS network's weights. Each weight is adjusted in the direction of the negative gradient, tempered by some learning rate γ that stabilizes convergence by scaling the step size according to the application at hand:

$$\Delta \mathbf{W}^{(h)} = -\gamma \frac{\partial E}{\partial \mathbf{W}^{(h)}} \tag{A10}$$

Once all weights are updated, the training epoch is complete. This procedure is repeated iteratively until the loss function converges.

3 Additional Information on Accuracy Tests

3A MAR-1 Experiment

Figure A1. Coverage of Complete-Data Coefficients Across Trials of MAR-1 Simulation Experiment

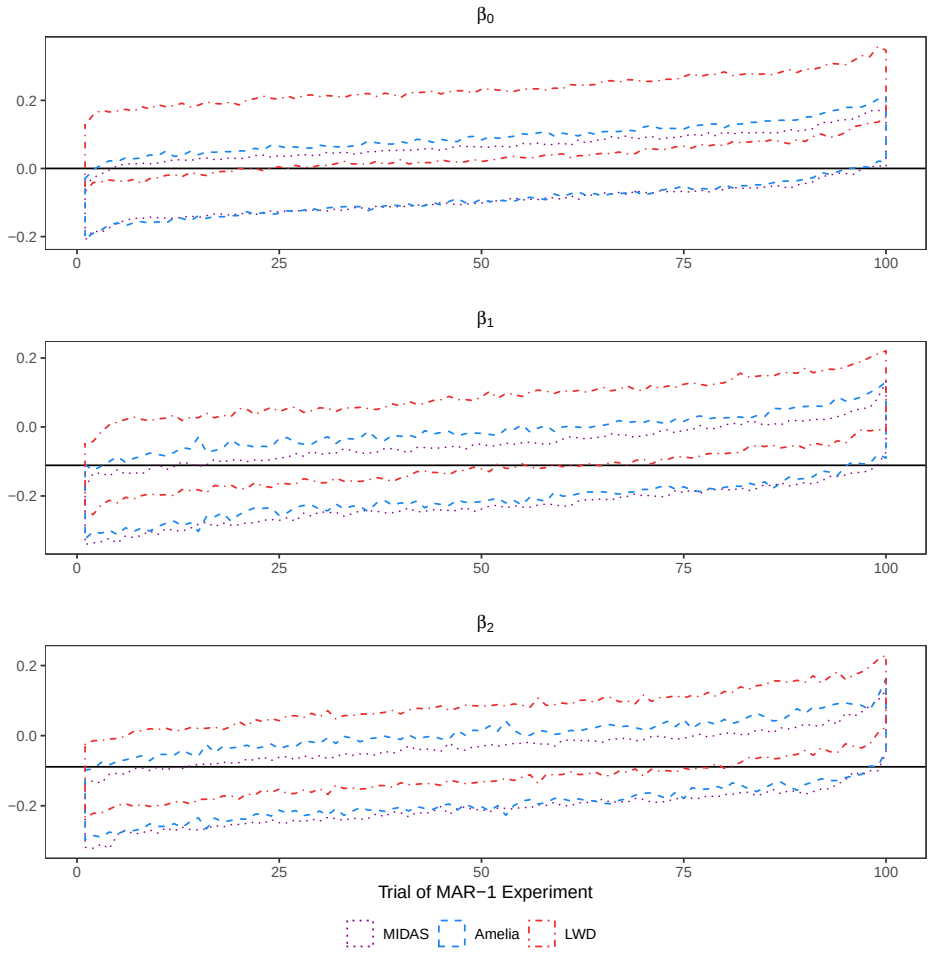

The solid black lines indicate complete-data ("true") coefficients in the MAR-1 experiment. The dashed lines represent 95% confidence intervals for each method's coefficient estimates across the 100 trials of the experiment (whose densities are plotted in Figure 3 in the main text).

Figure A1 plots the estimated confidence intervals produced by MIDAS, **Amelia**, and list-wise deletion across the 100 trials of the MAR-1 experiment. Similarly to the posterior densities of the estimated coefficients (Figure 3 in the main text), the **Amelia** and MI-

DAS intervals both exhibit good coverage for all three coefficients, encompassing the true estimate with a probability close to the ideal of 0.95.[2] Listwise deletion's coverage is substantially worse in every case, excluding this estimate — and hence failing to appropriately capture uncertainty — in at least 40% of simulations for two of the three coefficients (β_0 and β_1).[3]

3B Applied Test with Adult Dataset

Table A1. Summary Statistics for Adult Dataset

Variable	Type	Missing	Distribution	Description
class_labels (outcome)	Binary	0	>50K: 11,687; ≤50K: 37,155	Annual income
age	Continuous	0	Mean = 38.64; SD = 13.71	Age
workclass	Unordered categorical	2,799	Mode = Private (33,906); 7 other categories	Employment type
fnlwgt	Continuous	0	Mean = 189,664; SD = 105,604	Final weight (expected number in population)
education	Ordinal	0	Mode = HS-grad (15,784); 15 other categories	Highest level of education (categorical)
education_num	Continuous	0	Mean = 10.08; SD = 2.57	Highest level of education (numerical)
marital_status	Unordered categorical	0	Mode = Married-civ-spouse (22,379); 6 other categories	Marital status
occupation	Unordered categorical	2,809	Mode = Prof_speciality (6,172); 13 other categories	Employment sector
relationship	Unordered categorical	0	Mode = Husband (19,716); 5 other categories	Position in family
race	Unordered categorical	0	Mode = White (41,762)	Race
sex	Binary	0	Mode = Male (32,650); 1 other category	Sex
capital_gain	Continuous	0	Mean = 1079; SD = 7,452.019	Capital gains
capital_loss	Continuous	0	Mean = 87.5; SD = 403.00	Capital losses
hours_per_week	Continuous	0	Mean = 40.42; SD = 12.39	Hours worked per week
native_country	Unordered categorical	857	Mode = United-States (43,832); 41 other categories	Country of origin

The dataset has 48,842 rows representing individuals surveyed in the 1994 United States Census.

[2] **Amelia**'s coverage rates are marginally closer ($\beta_0 = 0.93$, $\beta_1 = 0.95$, $\beta_2 = 0.94$) to the ideal than MIDAS's ($\beta_0 = 0.93$, $\beta_1 = 0.86$, $\beta_2 = 0.87$), as should be expected under multivariate normal conditions.
[3] The coverage rates are $\beta_0 = 0.22$, $\beta_1 = 0.60$, $\beta_2 = 0.79$.

Table A2. Missingness Treatments Applied to Adult Dataset

Missingness Pattern	**Step**	**Procedure to Obtain R (Missingness Indicator Vector)**
MCAR	1.	Randomly select proportion of columns (0.3, 0.5, 0.7, or 0.9) for missingness treatment. $native\_country$, $occupation$, and $education$ cannot be selected (due to computational issues with **Amelia**).
	2.	$R \sim Bernoulli(p = 0.5)$ for each selected column.
MAR	1.	MCAR step 1.
	2.	L = one column randomly sampled from those *not* selected (latent missingness indicator).
	3a.	If L is continuous, select all rows with values at or below median of L. Sample N/2 rows from this matrix. For each selected column, $R_i = 1$ if row i's value is in this sample.
	3b.	If L is categorical, randomly sample half of all categories. If no. of rows in this matrix > 50% of N, sample N/2 of rows. For each selected column, $R_i = 1$ for all rows in remaining sample.
MNAR	1.	MCAR step 1.
	2.	L = selected column.
	3a.	If L is continuous, MAR step 3a.
	3b.	If L is categorical, select modal category. For each selected column, $R_i = 1$ for all except randomly sampled 5% percent of this sample.

4 Applied Accuracy Test on ANES Data

In addition to their multivariate normal simulation exercise (see Section 3.2 of the main text), Kropko et al. (2014a) conduct an applied accuracy test using the 2008 American National Electoral Studies (ANES) dataset. The ANES is, in theory, a good fit for MIDAS: like other electoral surveys, it is a wide and relatively diverse dataset, containing more than 1,000 columns (before any data transformations), many of which are categorical variables with large numbers of classes. Kropko et al., however, focus on a subset of the ANES comprising 11 columns — none of which present difficulties for existing MI algorithms (the categorical variables have few classes) — and the 1,442 complete observations in the dataset.[4] It thus offers another good opportunity to assess MIDAS's relative performance under statistical conditions that are well suited to existing MI algorithms.

In the first step of the test, ordinal variables are transformed into continuous integer-valued variables, binary variables are recoded to 0/1 format, and nominal variables are one-hot encoded. MAR missingness is then simulated in 10 percent of observations, excluding one column per data type, and five completed datasets are generated. The test consists of 20 simulations, across which the two accuracy metrics in Kropko et al.'s multivariate normal simulation are averaged.[5]

We instantiate MIDAS with a three-layer, 512-node network, which we train for 20 epochs. To ensure consistency across missing-data strategies, we make a few minor modifications to the test. First, we supply the one-hot encoded versions of the nominal variables to the marginal draws and **mi**-based strategies, which renders the multinomial logit (labeled "MI:MNL" by Kropko et al.) and renormalized logit ("MI:RNL") variants of the latter indistinguishable. Second, after imputation, we do not convert non-integer predicted prob-

[4]For detailed information on these variables, see Table 1 in Kropko et al. (2014a).
[5]Our description and extension of the test follow the code in Kropko et al.'s replication materials (Kropko et al. 2014b); their article reports a higher number of simulations.

abilities of binary and nominal variables into realized values through draws from further random distributions. This practice can lead to misleading results because the random draws may end up generating realized values with low predicted probabilities, resulting in large imputation error. Consequently, we maintain the raw predicted probabilities when comparing strategies.[6]

As in our applied accuracy test (Section 3.3 of the main text), we do not replicate the model-based component of the test because we do not know the true joint distribution of the data. Furthermore, since missingness in the original ANES is not completely random (according to Little's (1988) standard test), the parameters of a model estimated on the test subset may be nontrivially biased.

Figure A2 plots the average RMSE of imputed values generated by each strategy across the 20 completed datasets simulated in the test. Consistent with the results of our other accuracy tests, MIDAS's imputed values are more accurate than those of the remaining strategies for all 11 variables. This gap is particularly sizable for the nominal *religion* variables, where MIDAS's error is approximately 25% lower than that of every other strategy. It is worth reiterating, moreover, that this test presents favorable conditions for existing MI strategies; were it to be run on a wider subset of the ANES, MIDAS's (relative) performance would likely improve further.

[6]This is not possible in the case of **mi**, which automatically converts imputed values of binary variables to 0 or 1.

Figure A2. Inverse Imputation Accuracy in Kropko et al. Applied ANES Test

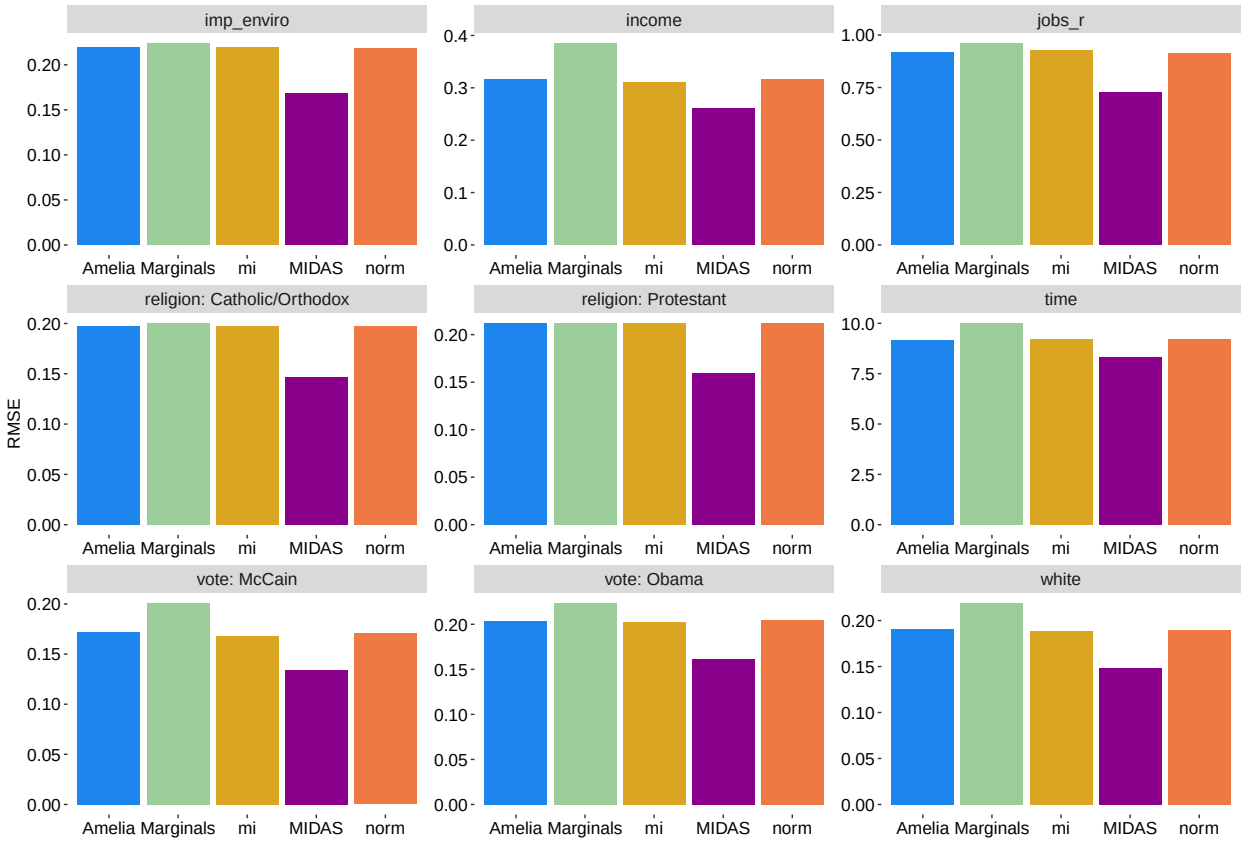

Lower RMSE indicates worse average imputation accuracy across the 20 completed datasets simulated in the test. Nominal variables (*vote*, *religion*) are one-hot encoded, with the residual category omitted. Ordinal variables (*income*, *jobs_r*) are transformed to continuous variables prior to imputation and not converted back subsequently. *female*, *age*, *education*, *married* are kept complete across simulations.

5 Additional Information on Scalability Analysis

5A List of Variables in Column-Wise Test

Binary *gender, pew_bornagain, cit1, investor, trans, votereg, edloan, CC18_417a_1, CC18_417a_2, CC18_417a_3, CC18_417a_4, CC18_417a_5, CC18_417a_6, CC18_417a_7, CC18_417a_8, CC18_418a, CC18_414A, CC18_414B, CC18_414C, CC18_414D, CC18_414E, CC18_324a, CC18_324b, CC18_324c, CC18_324d, CC18_415a, CC18_415b, CC18_415c, CC18_415d, CC18_416, CC18_417_a, CC18_417_b, CC18_417_c, CC18_417_d, CC18_417_e, healthins_1, healthins_2, healthins_3, healthins_4, healthins_5, healthins_6, healthins_7, CC18_300_1, CC18_300_2, CC18_300_3, CC18_300_4, CC18_300_5, CC18_300_6, CC18_303_1, CC18_303_2, CC18_303_3, CC18_303_4, CC18_303_5, CC18_303_6, CC18_303_7, CC18_303_8, CC18_303_9, CC18_303_10, CC18_303_11, CC18_320a, CC18_320c, CC18_320d, CC18_321a, CC18_321b, CC18_321c, CC18_321d, CC18_322a, CC18_322b, CC18_322c_new, CC18_322d_new, CC18_322c, CC18_322f, CC18_325a, CC18_325b, CC18_325c, CC18_325d, CC18_325e_new, CC18_325f_new, CC18_326, CC18_327a, CC18_327c, CC18_327d, CC18_327e, CC18_328b, CC18_328d, CC18_328e, CC18_328f, CC18_331a, CC18_331b, CC18_331c, CC18_332a, CC18_332b, CC18_332c, CC18_332e*

Categorical *sexuality, educ, race, employ, internethome, internetwork, marstat, pid3, religpew, ownhome, urbancity, immstat, union_coverage, unionhh, CC18_309a, CC18_309b, CC18_309c, CC18_309d, CC18_316, CC18_318a, CC18_335, CC18_350*

Ordinal *pew_religimp, pid7, ideo5, pew_churatd, pew_prayer, newsint, faminc_new, CC18_421a, CC18_app_dtrmp_post, CC18_422a, CC18_422b, CC18_422c, CC18_422d, CC18_422e, CC18_422f, CC18_422g, CC18_426_1, CC18_426_2, CC18_426_3, CC18_426_4, CC18_426_5, CC18_427_a, CC18_427_b, CC18_427_c, CC18_427_d, CC18_302*

Continuous *birthyr, citylength_1*

5B List of Variables in Row-Wise Test

Binary *gender, pew_bornagain, cit1, investor, trans, votereg*

Categorical *sexuality, educ, internethome, internetwork, marstat, pid3, ownhome, urbancity, immstat, unionhh*

Ordinal *pew_religimp, pid7, ideo5, pew_churatd, pew_prayer, newsint, faminc_new*

Continuous *birthyr, citylength_1*

6 Additional Information on Latent Ideology Estimation

6A List of Policy Questions

As discussed in the main text, we estimate CCES respondents' latent ideology by regressing their ideological self-placement on their answers to 19 policy questions in the survey. The former is based on CCES question CC18_334A (*Ideological Placement — Yourself*): "How would you rate each of the following individuals and groups?" Response options range from 1 for "Very Liberal" to 7 for "Very Conservative." The 19 policy variables are listed in Table A3.

6B Comparison with Amelia

Although existing MI algorithms cannot accommodate the full CCES sample on which we train the MIDAS imputation model, some of them can handle small subsets of this sample

Table A3. List of CCES Policy Variables Included in Latent Ideology Estimation

Variable	Policy.Area	Response.Type	Missing
CC18_414A	Minimum Wage	For/Against	8202
CC18_414B	Millionaire's tax	For/Against	8216
CC18_414C	Sales tax	For/Against	8233
CC18_414D	Income tax	For/Against	8230
CC18_414E	Abortion spending	For/Against	8223
CC18_324a	Government Spending	Support/Oppose	8304
CC18_324b	Government Spending	Support/Oppose	8324
CC18_324c	Government Spending	Support/Oppose	8298
CC18_324d	Government Spending	Support/Oppose	8280
CC18_415a	Carbon Dioxide regulation	Support/Oppose	8517
CC18_415b	Fuel efficiency regulation	Support/Oppose	8499
CC18_415c	Renewable energy policy	Support/Oppose	8476
CC18_415d	EPA powers	Support/Oppose	8456
CC18_416	Financial regulation	Support/Oppose	8495
CC18_426_1	State welfare spending	Increase/Decrease (1-5)	8311
CC18_426_2	State healthcare spending	Increase/Decrease (1-5)	8330
CC18_426_3	State education spending	Increase/Decrease (1-5)	8353
CC18_426_4	State law enforcement spending	Increase/Decrease (1-5)	8380
CC18_426_5	State transportation/infrastructure spending	Increase/Decrease (1-5)	8364

that exclude categorical variables with a large number of levels. Importantly, however, some of these omitted variables — such as respondents' state of residence and religion — are likely to be strong predictors of both the policy items and missingness in these variables. When they are excluded from the imputation model, therefore, estimates of latent ideology will tend to be closer to those based on listwise deletion.

To illustrate this point, we estimate latent ideology using a subset of the CCES data with the **Amelia** package in R. Specifically, we include five demographic variables — gender, sexuality, race, sector of employment, and party identification — in addition to the 19 policy variables included in the regression model (Equation 8).[7] As with MIDAS, we then generate 15 completed datasets and recover latent ideology estimates from the fitted

[7]We exclude several demographic variables with a higher number of categories to enable convergence.

Figure A3. Comparison of Latent Ideology Estimates from Different MI Strategies

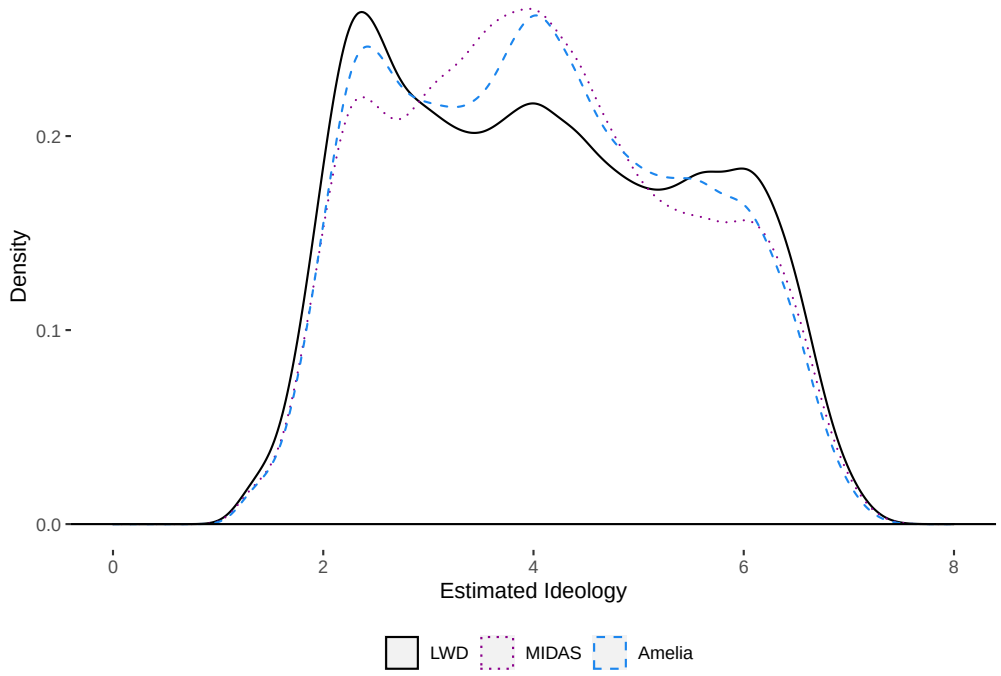

values of the regression.

Figure A3 plots the latent ideology estimates from listwise deletion, MIDAS, and **Amelia**. As expected, **Amelia**'s estimates are substantially closer to the listwise deletion estimates than MIDAS's. While the modal category is 4, there is a more pronounced peak on the left (liberal) side of the ideology scale and a flatter tail on the right (conservative) side. Compared to MIDAS, therefore, **Amelia** yields estimates with a clearly more peaked and less normal shape. We can reject the null hypothesis that the three sets of estimates are drawn from the same distribution at the $p < 0.01$ level in Kolmogorov-Smirnov tests.

These inferential differences are also significant from a practical perspective. In real datasets such as the CCES, the pattern and specific determinants of missingness are not known. The best option for users of MI is to leverage as much predictive information about the missingness mechanism and incomplete variables as possible. MIDAS enables us to utilize considerably more such information than existing MI strategies — with no

loss in imputation speed or accuracy — reducing the risk of bias and increasing statistical efficiency.

7 Imputing Time-Series Cross-Sectional Data: An Illustration

Finally, this appendix provides an illustration of MIDAS's ability to handle a particularly common type of non-exchangable data in social science research: time-series cross-sectional data.[8] As Honaker and King (2010) note, the dominant approach to MI tends to perform poorly with such data, yielding imputed values that are implausible based on substantive knowledge or that deviate substantially from previous and subsequent observations in a smoothly varying time series. These problems arise because the approach "assumes that the missing values are linear functions of other variables' observed values, observations are independent conditional on the remaining observed values, and all the observations are exchangable in that the data are not organized in hierarchical structures" (Honaker and King 2010, 565).[9] Although MIDAS — like most MI strategies — does not include any special functionalities for non-exchangable data, we have found that its capacity to learn complex relationships among variables enables it to accurately impute values in time-series cross-sectional settings with only small adjustments to the imputation model.

Building on an experiment conducted by Honaker and King (2010, 565-569) with **Amelia**, we demonstrate this capacity using data from the World Bank's World Development Indicators (WDI), a collection of almost 1,600 time-series indicators of social and economic development covering 217 countries since 1960.[10] We select six African countries — Cameroon, Côte D'Ivoire, Congo Republic, Ghana, Niger, and Zambia — over the

[8] Data are non-exchangeable if observations cannot be reordered without altering their joint distribution. More formally, a sequence of random variables $X_1, X_2, ..., X_n$ is non-exchangeable if its joint distribution is not identical to that of any (finite) permutation of its indices: $p(X_1, X_2, ..., X_n) \neq p(X_{\pi(1)}, X_{\pi(2)}, ..., X_{\pi(n)})$.

[9] **Amelia** seeks to avoid these problems by allowing users to construct a general model of temporal patterns with a sequence of polynomials of the time index. Such a sequence could, of course, be included in a MIDAS model.

[10] `http://datatopics.worldbank.org/world-development-indicators/`.

period 1970-2000, drop all entirely missing columns, and sequentially remove a single country-year observation of GDP (measured in constant 2010 United States dollars) from each cross-section (31 years $\times$ six countries).[11] This yields 186 different subsets of the WDI, each comprising 186 observations and 1251 variables — samples that are too wide for any existing MI algorithm to process. Note, however, does this setup does not play to MIDAS's strengths either, given that the accuracy of neural networks generally increases with the number of observations.

For each sample, we generate lags and leads of all (non-index) variables, since both past and future values of a given variable tend to be correlated with its present value (Honaker et al. 2011, 19). Based on an overimputation analysis (see Section 1), we instantiate MIDAS with two hidden layers of 1024 and 512 nodes, a learning rate of $3e-5$, a dropout rate of 0.95, and 2000 training epochs. We include country dummies as well as the lags and leads in the imputation models, bringing the total number of variables to 3756.[12] 200 completed datasets are then produced with each model.

Figure A4 compares real versus MIDAS-imputed values of GDP for the six countries. In general, the latter data track the former remarkably closely through each time series, even capturing trends that were missed by **Amelia**, such as Côte d'Ivoire's cocoa crisis in the late 1970s and Cameroon's strong economic recovery in the mid-1980s (Honaker and King 2010, 569). Only a handful of real values fall outside the interquartile range of MIDAS's imputations, most of which are at the extremities of the time series. This is probably a consequence of the absence both of lags at the beginning of the time series and of leads at the end. Incorporating into the imputation model data from shortly before and after the time period of interest — if available — may help to avoid this problem.

[11] We deviate from Honaker and King's selection of countries by substituting Niger for Mozambique, since the latter lacks a complete GDP time series in the WDI.

[12] Given the large number of imputation models in this exercise, we pass all variables other than country, year, and GDP to the `additional_data` argument in MIDAS, which excludes them from the cost function and hence accelerates training.

Figure A4. Real Versus MIDAS-Imputed GDP for Six African Countries, 1970-2000

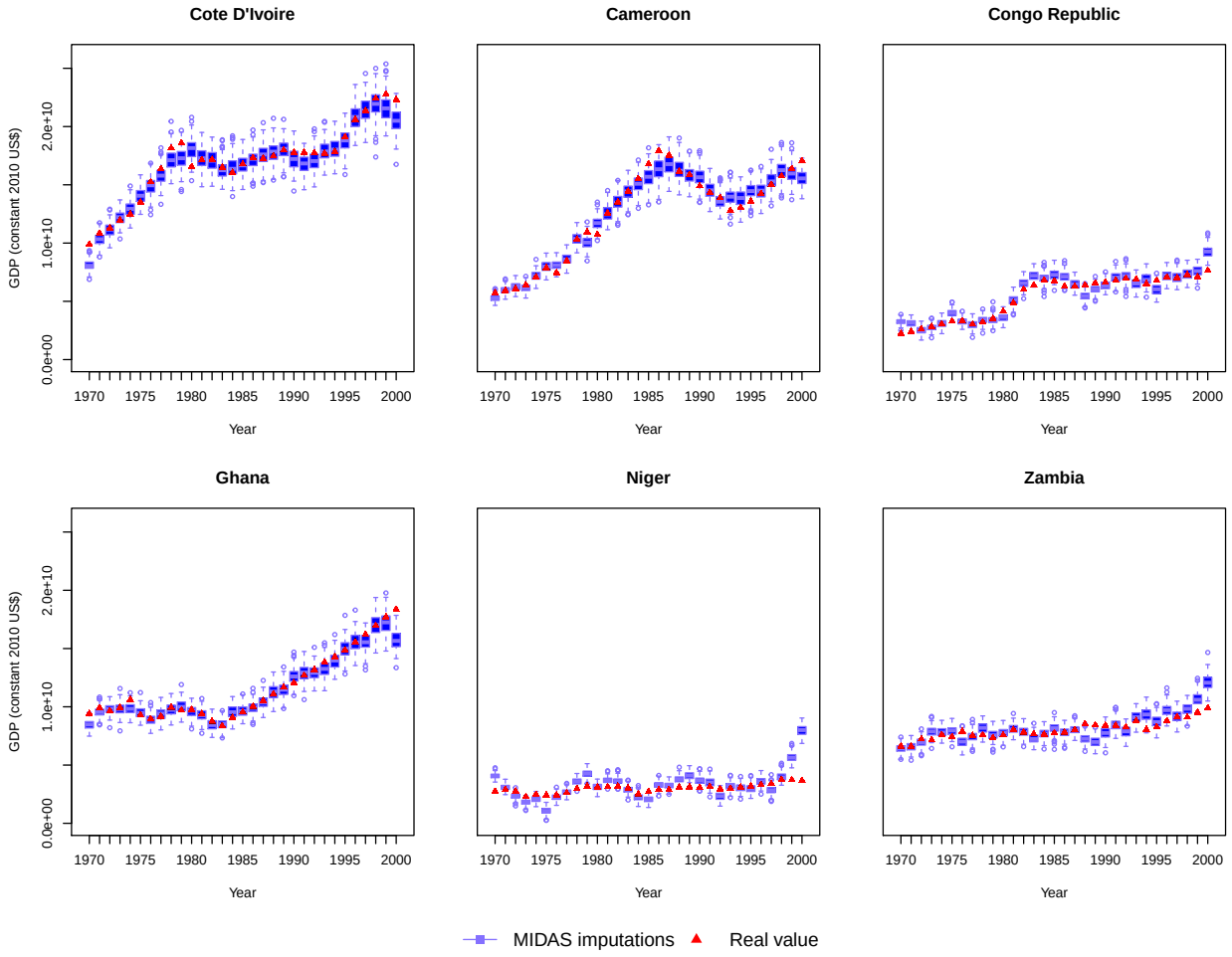

MIDAS imputations are based on variants of the WDI dataset in which country-year observations of GDP are sequentially removed. Each imputation model includes all variables in the WDI that are not entirely missing for the six countries, leads and lags of all non-index variables, and country dummies.

In sum, MIDAS can successfully recover smooth temporal trends in GDP for all six countries. This is particularly notable in light of the absence of explicit features for modeling time and the high ratio of variables to observations, which often leads to poor imputation accuracy with existing MI strategies. To be sure, MIDAS would not perform as well in the presence of longer periods of missingness and sharper inflection points in the time series. However, provided that the imputation model contains sufficiently rich information about

how observed values are related at different points in time, posterior uncertainty should be low enough to permit valid statistical inference. The inclusion of additional features in the model, such as polynomials of the time index and flexible basis functions, could further improve MIDAS's performance.

References

Blackwell, M., J. Honaker, and G. King (2017). A unified approach to measurement error and missing data: Overview and applications. *Sociological Methods & Research 46 (3)*, 303–341.

Christiansen, B. (2005). The shortcomings of nonlinear principal component analysis in identifying circulation regimes. *Journal of Climate 18*(22), 4814–4823.

Goodfellow, I., Y. Bengio, and A. Courville (2016). *Deep Learning*. Cambridge, MA: The MIT Press.

Honaker, J. and G. King (2010). What to do about missing values in time-series cross-section data. *American Journal of Political Science 54 (2)*, 561–581.

Honaker, J., G. King, and M. Blackwell (2011). Amelia II: A program for missing data. *Journal of Statistical Software 45 (7)*, 1–47.

Kingma, D. P. and M. Welling (2013). Auto-encoding variational bayes. *ArXiv e-prints*.

Kropko, J., B. Goodrich, A. Gelman, and J. Hill (2014a). Multiple imputation for continuous and categorical data: Comparing joint multivariate normal and conditional approaches. *Political Analysis 22 (4)*, 497–219.

Kropko, J., B. Goodrich, A. Gelman, and J. Hill (2014b). Replication data for: Multiple Imputation for Continuous and Categorical Data: Comparing Joint Multivariate Normal and Conditional Approaches.

Little, R. J. (1988). A test of missing completely at random for multivariate data with missing values. *Journal of the American Statistical Association 83 (404)*, 1198–1202.

Probst, P., A.-L. Boulesteix, and B. Bischl (2019). Tunability: Importance of hyperparam-

eters of machine learning algorithms. *Journal of Machine Learning Research 20*(53), 1–32.

Rezende, D. J., S. Mohamed, and D. Wierstra (2014). Stochastic backpropagation and approximate inference in deep generative models. In *International Conference on Machine Learning*, pp. 1278–1286. ACM.

Scholz, M. (2012). Validation of nonlinear pca. *Neural Processing Letters 36 (1)*, 21–30.